PX3A9 - Black Holes, White Dwarfs and Neutron Stars
Typed Module Notes

L.J. Aitchison

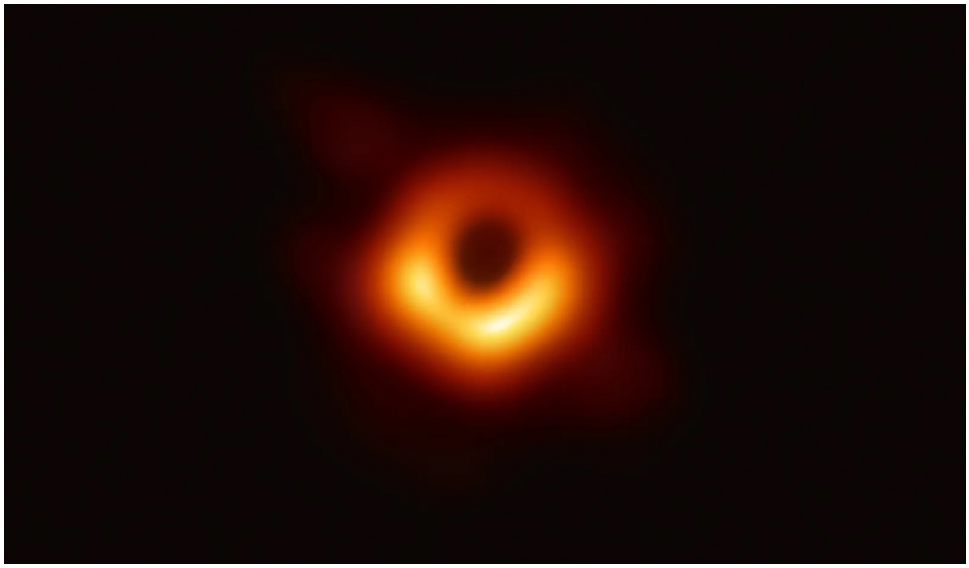

April 29, 2025

Contents

Introduction

This is a summary and revision document for the third year physics module PX3A9: Black Holes, White Dwarfs and Neutron Stars at the University of Warwick. It endeavours to cover the main parts of the module and all the relevant information, equations and discussions.

Disclaimer: No gurantee can be made that this document is complete or withour error. Please contact me with any suggestions or corrections you may have.

Acknowledgments: Many thanks to the lecturers Professor Deanne Coppejans and Professor Don Pollaco for supplying the enlightening diagrams and figures found throughout these notes as well as the handwritten notes that this typed set was adapted from.

1 Formation of Black Holes, White Dwarfs and Neutron Stars

1.1 Stellar Physics

1.1.1 Hydrostatic Equilibrium

To begin, we do a quick review of hydrostatic equilibrium. Consider a cylinder of mass dm in a star which is in hydrostatic equilibrium with its surroundings (i.e. the star is not expanding nor contracting). The two forces on the cylinder are gravity, which

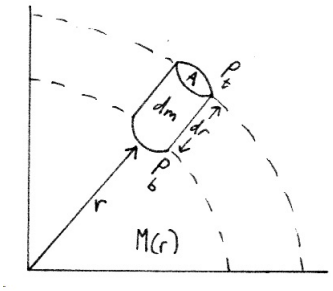

Figure 1: Cross-section of a star

acts radially inwards, and pressure, which acts radially outwards. The net force on the cylinder obeys Newton's second law, giving

$$F_{\text{net}} = ma = dm\frac{d^2r}{dt^2}$$

Moreover, by definition, we have

$$F_{\text{net}} = F_g + F_{p,t} + F_{p,b}$$

where F_g is the gravitational force and $F_{p,t}$ and $F_{p,b}$ refer to the pressure forces on the top and bottom of the cylinder respectively. We can rewrite this as a pressure differential as follows

$$F_{\text{net}} = F_g + dF_p$$

We also have the standard equation for gravitational force:

$$F_g = \frac{-GM(r)dm}{r^2}$$

and the standard equation for pressure which can be adapted to get the equation for the differential as such

$$F_p = PA \implies dF_p = AdP$$

Hence, setting these expressions equal we get

$$F_{\text{net}} = dm\frac{d^2r}{dt^2} = -\frac{GM(r)dm}{r^2} - AdP \quad (*)$$

If the cylinder has density ρ, we have

$$dm = \rho A dr$$

Substituting this in to $(*)$ gives

$$A\rho dr\frac{d^2r}{dt^2} = -\frac{GM(r)\rho A}{r^2} - AdP$$

Then, dividing by volume gives

$$\rho\frac{d^2r}{dt^2} = -\frac{GM(r)\rho}{r^2} - \frac{dP}{dr}$$

Assuming the star is static means the term on the left hand side of the equation is zero. Thus, the equation can be rearranged to give the following

$$\frac{dP}{dr} = -\frac{GM(r)\rho}{r^2}$$

which is the condition for **hydrostatic equilibrium**.
This demonstrates that a pressure gradient is required to counteract gravity and prevent the star from collapsing.

1.1.2 Pressure Gradient and Electron Degeneracy Pressure

There are multiple factors contributing to the overall pressure gradient. These are

(i) Ideal gas pressure

(ii) Radiation pressure

(iii) Electron degeneracy pressure

Electron degeneracy pressure is of particular importance to us in this module, so we will discuss it now. There is a fundamental physical limit to how densely one can pack electrons. This is as a result of **Pauli's exclusion principle** which states that two or more fermions cannot occupy the same quantum state. As the density of the stellar material increases, electrons are forced into lower energy levels. They cannot all be in this level, so electrons are stacked in the higher energy levels and their non-thermal motion creates a pressure. This is what we refer to as **electron degeneracy pressure**. The matter in this state is called **electron degenerate**.

It is important to note at this point that neutrons are also fermions and can form a **neutron degenerate material**. We will discuss this soon.

In most stars, except the ones we discuss in this module, ideal gas pressure dominates.

1.1.3 Sources of Energy

When consider stars and their eventual fate, it is important to understand the mechanisms behind the transfer of energy within them. There are two mains ones that we will consider.

The first one is **gravitational contraction**, which is the release of gravitational potential energy as the star contracts. The change in gravitational potential energy is given by the standard result

$$U = -\frac{GMm}{r}$$

Half of this energy is transferred to thermal energy as described by the Virial theorem encountered in previous astrophysics modules. The other half of the energy is radiated away by the star. Ergo, contraction increases the temperature of the star.

The other source of energy is **nuclear fusion**. We firstly define **binding energy**, which is the energy required to split the nucleus into its individual components. The binding energy per nucleon is given by the expression

$$\frac{\Delta mc^2}{A} = \frac{1}{A}\left([Zm_p + (A-Z)m_n - m_{\text{nucleus}}]\,c^2\right)$$

where A denotes the mass number (i.e. the number of protons and neutrons), Z denotes the number of protons, m_p denotes the mass of a proton and m_n denotes the mass of a neutron. Stars can fuse hydrogen into helium, helium into carbon and oxygen, carbon

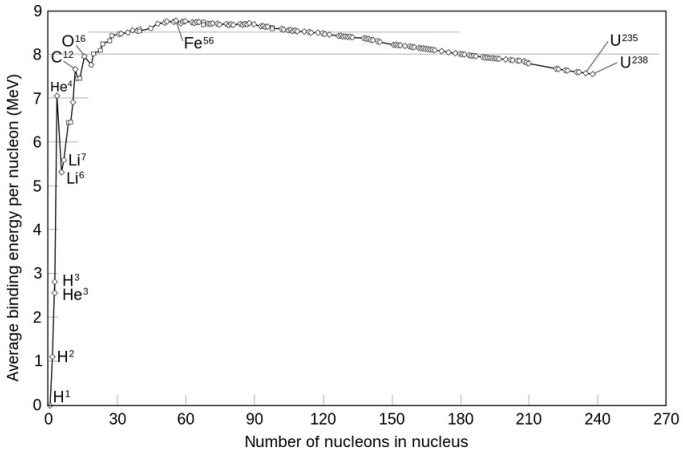

Figure 2: Binding energy curve

into silicon, sulphur, magnesium and phosphorous and silicon can then be fused into iron, cobalt and nickel. Once this point is reached, no further elements can be fused as to make heavier elements it is required to put energy in, as can be seen in Figure 2 above. Furthermore, the timescales for each fusing stage decreases rapidly to the point where the timescale for silicon fusion in a $20M_\odot$ star is approximately two days.

Higher temperatures are necessary to produce the temperatures necessary for the fusion of heavier elements but not all have a sufficient mass to *reach* the temperatures necessary to fuse these heavier elements. Ergo, the mass of a star determines which elements can fuse and what the evolution and endpoint of a star will be.

1.2 Stellar Evolution

1.2.1 Definitions

We now discuss a simplified model of stellar evolution. It is simplified as we will not be considering the cases where the core or parts of the shell are not fusing elements.[1]

To begin with, we define some terms we will be using:

[1]These details can be found in the second year module PX282 as well as in 'An Introduction to Modern Astrophysics' by Carroll and Ostlie.

- ZAMS will be an acronym we use to denote **zero age main sequence**, which is the point at which the star started fusing hydrogen.
- M_{ZAMS} will denote the mass at the start of hydrogen burning.
- **Core mass** is the mass of the inner stellar core (*not* including the envelope)
- **Compact objects** will refer to either white dwarfs, neutron stars or black holes

1.2.2 Timeline of Stellar Evolution

We will now go through several defining points of stellar evolution. In class, a handout was provided with a flowchart structure of these key sections. This has been provided in the appendix.

To begin, only objects with a mass of greater than $0.08\,\mathrm{M}_\odot$ can fuse hydrogen into helium (i.e. become stars). The core temperature required for this fusion is $T_c \geqslant 1 \times 10^7\,\mathrm{K}$. The structure of the star at this point is comprised of a core fusing hydrogen into helium, surrounded by an envelope of hydrogen. Over time, the star fuses hydrogen

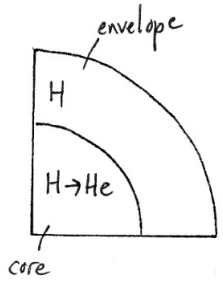

Figure 3: Cross-section of a Star

into helium until a time when the hydrogen in the core runs out. At this time, the energy output from fusion ceases and the force of gravity dominates, causing the star to contract. As a result the core temperature T_c increases. We now come to our first defining point: Is $M_{\text{ZAMS}} > 0.3\,\mathrm{M}_\odot$?

If it is **not**: Then the star has a helium core that is not hot enough to fuse, surrounded by the envelope of hydrogen. The outer layers then expand into a **planetary nebula**. This gas absorbs ultraviolet radiation from the hot core and emits optical light. The

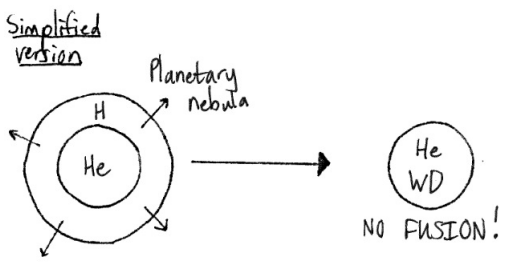

Figure 4: Case when $M_{\text{ZAMS}} < 0.3\,\mathrm{M}_\odot$

core that is left behind is a **helium white dwarf** (where *no fusion* is occurring). The collapse of this white dwarf is prevented by electron degeneracy pressure.

If the mass **is** high enough, then helium fusion can commence. In this case, the star consists of a core of helium fusing into carbon and oxygen, surrounded by a shell of hydrogen fusing into helium which is itself surrounded by a layer of hydrogen. As

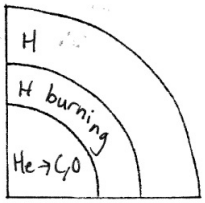

Figure 5: Helium fusing star

before, this cannot continue indefinitely. Therefore, when the star is depleted of helium to fuse the gravitational forces once again dominate and the star contracts, heating the core.

This brings us to our second defining point: Is $M_{\text{ZAMS}} > 7\,\text{M}_\odot$?

If it is **not**: A similar thing happens as in the previous case. The star is left with a carbon and oxygen core where the outer layers are blown away as a planetary nebula. This leaves behind a **carbon and oxygen white dwarf** which is again not fusing, instead by supported by electron degeneracy pressure. If the mass **is** high enough, then the core

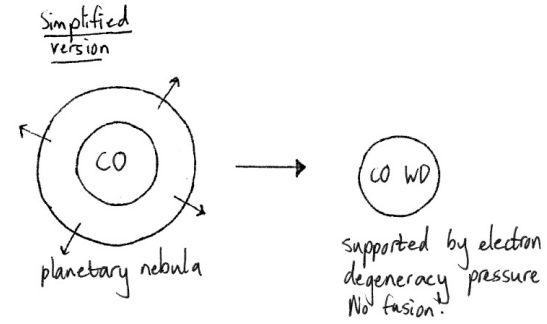

Figure 6: Case when $M_{\text{ZAMS}} < 7\,\text{M}_\odot$

temperature is able to rise above $6 \times 10^8\,\text{K}$ meaning that carbon fusion can commence. From here, a familiar thing occurs. The star comprises of a core of carbon fusing into neon, magnesium, oxygen and sodium surrounded by a layer of helium fusing, which is itself surrounded by a layer of hydrogen fusing, which is all surrounded by a further layer of hydrogen. The star eventually runs out of carbon in the core, resulting in the star contracting once again and the core temperature rising.

Here, we come to our third defining point: Is $M_{\text{ZAMS}} > 8\,\text{M}_\odot$?

If it is **not**: The same procedure occurs where the outer layers of the star are expelled leaving behind a neon, magnesium, oxygen white dwarf. The mass of this white dwarf is in the range of $1.1\,\text{M}_\odot$ up to $1.4\,\text{M}_\odot$. This upper bound is a key quantity that we will return to soon.

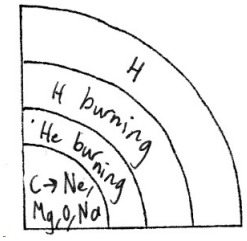

Figure 7: Carbon fusing star

At this eight solar mass consideration, we have reached a very important distinction when it comes to stars. If the star **is** greater than eight solar masses, then it is so heavy that it will be able to continue fusing elements up until iron (which we know from our previous discussion on nuclear binding energy is the limit). At this point, the star is so heavy that electron degeneracy pressure is no longer sufficient to halt its collapse. All stars beyond this mass will end in a catastrophic explosion known as a supernova. Ergo, we have the splitting that stars less than eight solar masses are called **low mass stars** which will go on to become *white dwarfs*, whilst stars greater than eight solar masses are called **high mass stars** which will go on to become *neutron stars* or *black holes*.

We are now at the point where oxygen and silicon have fused to create a star with the following structure: This is the *final* fusion product of a star with a (zero age main

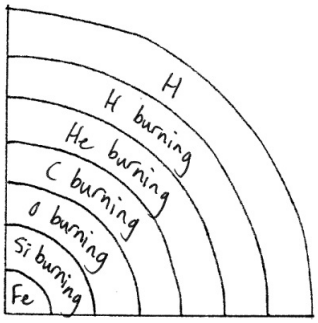

Figure 8: Iron core star

sequence) mass of greater than eight solar masses since, as previous mentioned, the fusion of iron is endothermic. From this point, iron begins to build up in the core. As there is no fusion occuring, the core is supported mainly by electron degeneracy pressure up until the iron core exceeds $1.4\,\mathrm{M}_{\odot}$. This is called the **Chandrasekhar mass** and is the upper limit for the mass of white dwarfs as beyond this, electron degeneracy pressure is unable to prevent the collapse of the core. Hence, in this case the iron core collapses until **neutron degeneracy pressure** halts said collapse. This creates a shockwave which blows off the outer layers of the star (a *supernova*).

We now come to our fourth and final defining point: Is $M_{\mathrm{ZAMS}} > 25M_{\odot}$?

If it is **not**: A *neutron star* is left behind, which is the old core of the former star. This object is supported by neutron degeneracy pressure. If the mass **is** greater than this limit, neutron degeneracy pressure is not sufficient to prevent the collapse of the core of the former star. This results in the collapse of the core into a singularity called

a *black hole*.

It is important to note that this is how white dwarfs, neutron stars and black holes are formed through *single star evolution*. However, binary interactions and mergers also form compact objects.

To summarise:

$$M_{\text{ZAMS}} \leqslant 8\,\text{M}_\odot \implies \text{White Dwarf}$$
$$8\,\text{M}_\odot \leqslant M_{\text{ZAMS}} \leqslant 25\,\text{M}_\odot \implies \text{Neutron Star}$$
$$25\,\text{M}_\odot \leqslant M_{\text{ZAMS}} \implies \text{Black Hole}$$

1.2.3 What fraction of stars become compact objects?

In order to consider this question, we need to examine an expression called the **initial mass function** or **IMF**. This is an empirical function shows the probability mass distribution of stars at the zero age main sequence. There are different IMFs[2] and we will consider one called the **Salpeter IMF**[3]. This gives us the number of stars in mass range m to $m+dm$ (within some volume) which is proportional to $m^{-2.35}$. The function is

$$\xi(m)\Delta m = \xi_0 \left(\frac{m}{M_\odot}\right)^{-2.35} \left(\frac{\Delta m}{M_\odot}\right)$$

where ξ_0 is a constant relating to the local stellar density. This tells us that vast majority of stars are low mass and so white dwarfs are very common - more than 90% of stars form white dwarfs. On the other hand, high mass stars are quite rare and so only a few supernovae are seen per *galaxy* every one hundred years.

1.3 (Core-collapse) Supernovae

In the previous subsection, we noted that any star with a mass greater than eight solar masses end its life in an extreme explosion known as a supernova. We now want to analyse and discuss these events.

Recall that prior to a supernova, we have an iron core that is not able to fuse. This core is mainly supported by electron degeneracy pressure. This iron core continues to grow and eventually becomes too massive to be supported by electron degeneracy pressure, resulting in core collapse. However, pressure in the core is also being decreased by other mechanisms.

The first of these is **photo-disintegration**, where at the extremely high temperatures within the core the photons are energetic enough to destroy heavy nuclei. This occurs by the following reactions

$$^{56}_{26}\text{Fe} + \gamma \longrightarrow 13\,^{4}_{2}\text{He} + 4\,\text{n} - 100\text{MeV}$$

then

$$^{4}_{2}\text{He} + \gamma \longrightarrow 2\,\text{p}^{+} + 2\,\text{n} - 25\text{MeV}$$

This process is highly endothermic and so removes a significant amount of thermal energy that was helping to support the core.

[2] Other IMFs include the Miller-Scalo (1979), Kroupa (2002) and Chabrier (2003)

[3] Developed by Austrian-Australian-American physicist Edwin Ernest Salpeter (1924-2008)

The second is **electron capture** and **neutrino release**. At these temperatures and pressures, electrons that were supporting the star through degeneracy pressure are caputed by heavy nuclei as well as the protons produced by photo-disintegration in the following way

$$\mathrm{p}^+ + \mathrm{e}^- \longrightarrow \mathrm{n} + \nu_e$$

where ν_e is an **electron neutrino**. These are electrically neutral particles that have an incredibly small mass and interaction cross section. This means they very easily escape the star, resulting in enormous amounts of energy loss.
Through these two mechanisms, most of the support of the core is removed and so the inevitable collapse is accelerated.

1.3.1 Process of a Supernova

We now have an extremely rapid collapse of a core of a former star under gravity and the process of a supernova is well underway. At the radius where the collapse velocity exceeds the local sound speed, the collapse itself cannot remain homologous and so the inner core collapses at a faster rate. This inner collapse happens at such a great speed that the outer layers of the former star are left suspended around the core.

The core itself is converted to neutrons through photo-disintegration and electron capture. The collapse continues until the density reaches about three times the density of a nucleus, at which point the strong force becomes repulsive resulting in the creation of neutron degenerate material.

The core effectively 'bounces' at this point, sending a shockwave outwards throughout the outer core (which is still collapsing inwardly). The shockwave heats the surrounding gas resulting in more photo-disintegration and subsequently stalls. However, the material near this shock is so dense that not all the neutrinos are able to escape. This results in $\sim 5\%$ of the neutrino energy being deposited behind the shock, resulting in a heating of the material. This enables the shock to restart.

This restarted shock travels outwards, ionising material and producing radioactive nickel among other elements heavier than iron. Furthermore, this shock blows off the outer layers of the star at around ten percent the speed of light. This shockwave takes a variable time to travel through the star (on the scale of minutes to days) depending on its radius.

These expanding ejecta 'glow' massively through recombination and the deposition of energy via radioactive decay. At its peak, this is about ten billion times more luminous than the sun and can outshine entire galaxies - this is primarily how they are spotted by astronomers.

Recall that what happens to the core depends on its zero age main sequence mass: If it is less than $25\,\mathrm{M}_\odot$, neutron degeneracy pressure halts the collapse and a neutron star is left but if it is greater than $25\,\mathrm{M}_\odot$ then nothing is able to halt the collapse and a black hole is formed.

In the majority of cases, the outflow of material is approximately spherical. However, in the case of the most massive, rapidly rotating stars extremely energetic supernovae more distinctive formations can occur. These include highly magnetic and rapidly spinning neutron stars and black holes surrounded by a disk of (stellar) material. This type of black hole accretes the surrounding material and launches highly relativistic streams of matter called **jets**. This is called the **collapsar model** and as the jets it describes punches through the material, the induced shocks radiate gamma rays for longer than two seconds. These radiations are called **long gamma ray bursts**.

1.3.2 Energetics of a Supernova

As huge amounts of energy are involved in these events, it is important to consider where it is being transferred. In order to do this we will focus on the iron core that lay at the heart of the former star. For some typical values, take the mass of the core $M_c \approx 1.4 M_\odot$ and its radius to be $R_c \approx 7 \times 10^6$ km which is collapsing to a size of about 1×10^4 m.
The energy of a supernova comes from gravitational potential energy being released during collapse. This can be calculated by

$$\Delta E_G = -GM_c^2 \left(\frac{1}{R_c} - \frac{1}{R_{NS}} \right) \simeq 5 \times 10^{46}\,\text{J}$$

Firstly, this energy is abosrbed in nuclear processes whose proportion is calculated by

$$\Delta E_N = 7(\text{MeV}) \frac{M_c}{M_H} \simeq 2 \times 10^{45}\,\text{J}$$

which accounts for about 4% of the energy. Next, we have energy released as electromagnetic radiation which is calculated by multiplying the luminosity of the supernova by its lifetime. A typical value is

$$E_{\text{rad}} \simeq 3 \times 10^{44}\,\text{J}$$

or 0.6 % of the available energy. There is also the energy transferred to the kinetic energy of the ejecta, given by

$$\Delta E_k = \frac{1}{2}(M_* - M_c) v_{\text{ej}}^2 \simeq 9 \times 10^{44}\,\text{J}$$

accounting for another 2% of the energy. Moreover, there is the energy involved in 'unbinding' the envelope surrounding the core, calculated by

$$\Delta E_{\text{env}} = GM_c \frac{(M_* - M_c)}{R_c} \simeq 5 \times 10^{44}\,\text{J}$$

which is another 1% of the total energy.

Notice that this only accounts for $\sim 7.6\,\%$ of the total energy involved. The vast majority of the energy is in fact transferred away via the neutrinos produced in the supernova. There are about 10^{57} neutrinos being released in under a second(!)

1.3.3 Classification of Supernovae

As stated in the title of the subsection, supernovae of the type just discussed are called *core-collapse supernovae*. However, there is also a *thermonuclear supernova* which we will discuss later in the course.

Naturally, we want a way of classifying supernovae. The system that is used is purely based on the elements seen in the expanding sphere of gas ejected by the late star. The following diagram demonstrates what type of supernova corresponds to which

elements:

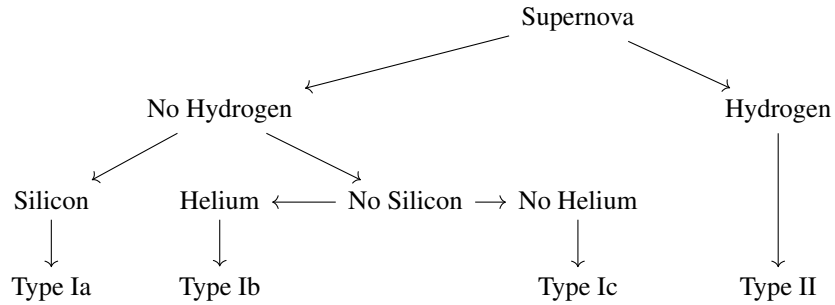

Here, type Ia supernovae are the **thermonuclear** variants that will be explored later in the course, whilst type Ib, Ic and II are all the **core-collapse supernovae** that have the process we discussed previously.

2 Physics of Degenerate Matter

We are now aware of how the compact objects we wish to consider form. Developing upon this, we now seek to analyse the constituents of these objects.

2.1 Equation of state for Electron Degenerate Matter

In stars, the equation of state (which is a relation between pressure and density) is polytropic. This equation of state will take the form

$$P = K\rho^{\frac{n+1}{n}}$$

where K is a constant and n is an integer that will vary depending on the star. From this relation, we are able to calculate many key properties of the star and so it is of critical importance to our understanding of these compact objects.
To begin, we will consider the plot below

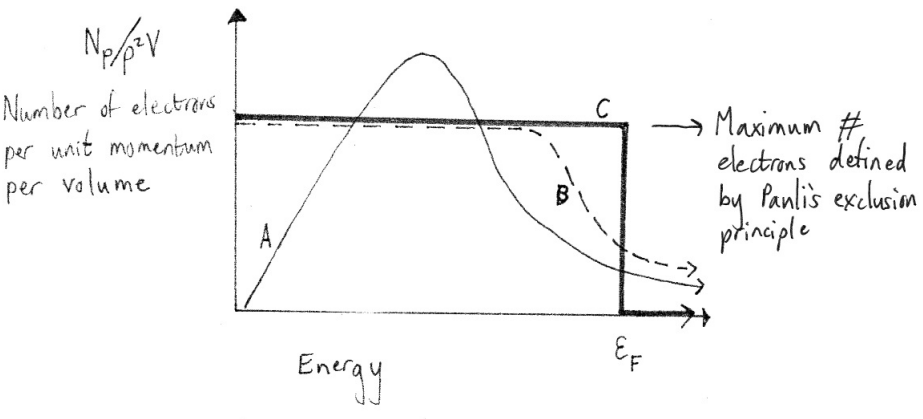

Figure 9: Particle-Energy Distribution

The key points are as follows:

- Curve **A** describes an ideal gas with a Maxwellian particle distribution. In this material, thermal pressure is related to pressure via the ideal gas law and is *not* degenerate.
- Curve **B** describes a partically electron degenerate gas. Matter cannot be contiually compacted into smaller and smaller volumes, as eventually more than one electron would have to be in each quantum state thereby violating Pauli's exclusion principle.
- Curve **C** describes a completely degenerate gas at 0 K. Here, the electrons fill all the lower energy states until a certain value, called the **Fermi energy** ε_F, is reached. This value is maximum possible energy of an electron in a completely degenerate gas at 0 K.

The Fermi energy described above can be expressed as

$$\varepsilon_F = \frac{h^2}{2m_e}(3\pi^2 n_e)^{\frac{2}{3}}$$

where m_e is the mass of an electron and n_e is the number of electrons per unit volume.

2.1.1 Derivation of the Electron Degeneracy Pressure

In order to calculate the electron degeneracy pressure, we require a few things. We need to know:

- How many electrons there are in the volume we are considering. With regards to this, remember that an electron degenerate material is being considered and so we need to instead be considering **how many quantum states there are** per unit volume.
- The momentum of these electrons

The quantum state of an electron is given by the values that describe its position and momentum (i.e. in cartesian coordinates the values $[x, y, z, p_x, p_y, p_z]$ are needed). Heisenberg's uncertainty principle, usually given by

$$\Delta x \Delta p \geqslant \frac{h}{4\pi}$$

determines the limit of how well we can know any of these simultaneously. It is important to visualise these concepts clearly, so instead of thinking of a quantum state as a point in this six-dimensional position-momentum space, called **phase space**, it is more beneficial to think of a quantum state as a volume h^3 of this phase-space. When considering a degenerate gas, we know that by Pauli's exclusion principle each volume h^3 in this space is occupied by two electrons (one spin up and one spin down). This is shown in the diagram below, along with the familiar position and momentum spaces.

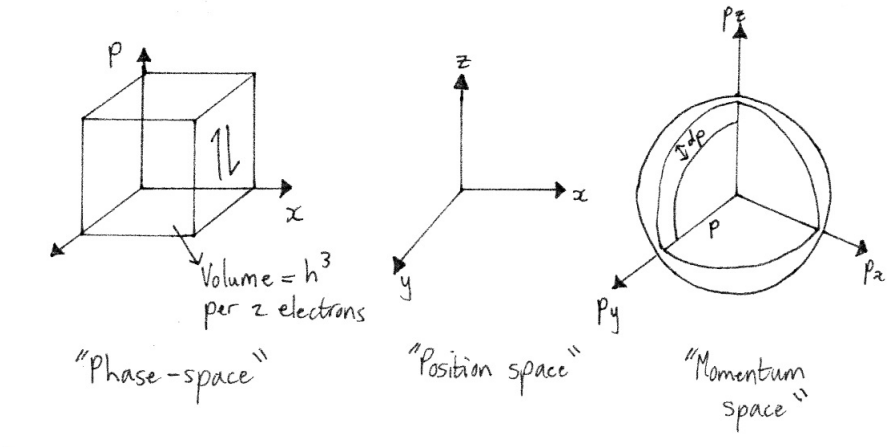

Figure 10: Different spaces

In our derivation, we will move between these three spaces.

Our starting point is the **pressure integral**, given as

$$P = \frac{1}{3}\int_0^\infty N_p p v \ \ dp$$

where N_p refers to the number of particles per unit volume. Consider a sample of electrons with momentum in the range p to $p+dp$ which occupy a volume V in position-space. The corresponding volume of phase-space occupied will be equal to the volume in position-space *multiplied* by the volume in momentum-space. We know that the momentum-space volume V_p is

$$V_p = 4\pi p^2 dp$$

Hence, the volume of phase-space is given by

$$V_{PS} = 4\pi p^2 dp \cdot V$$

Therefore, the number of quantum states is given by

$$\#\text{QS} = \frac{4\pi p^2 V}{h^3} dp$$

as it is the volume of the phase-space divided by the volume of a quantum state. The number of electrons in this volume is then determined by

$$N_e dp = \frac{8\pi p^2 V}{h^3} dp$$

where N_e denotes the number of electrons per unit momentum. Notice that the extra factor of two has arisen since we have both one up and one down electron and so two per state.

In a completely degenerate gas which is at 0K, all momentum states up to some critical value p_0 are filled. Thus,

$$N_e = \begin{cases} \frac{8\pi p^2 V}{h^3} & \text{if } p \leqslant p_0 \\ 0 & \text{if } p > p_0 \end{cases} \tag{1}$$

By integrating over this value, we get the total number of electrons in the volume V. Therefore, we now have the expression for the number of electrons as

$$N = \frac{8\pi V}{h^3}\int_0^{p_0} p^2 dp = \frac{8\pi p_0^3 V}{3h^3} \tag{2}$$

Next, we need a relation between p and v. We are considering a densely packed relativistic gas and so we have the standard expression from special relativity

$$p = \gamma m_e v = \frac{m_e v}{\sqrt{1-\left(\frac{v}{c}\right)^2}}$$

which can be rearranged to get

$$v = \frac{p}{m_e}\left(1+\frac{p^2}{m_e^2 c^2}\right)^{-\frac{1}{2}} \tag{3}$$

Therefore, by inserting (1) and (3) into the pressure integral we obtain an expression for the pressure of a completely degenerate gas, namely

$$P = \frac{8\pi}{3h^3 m_e} \int_0^{p_0} \left[p^4 \left(1 + \frac{p^2}{m_e^2 c^2} \right)^{-\frac{1}{2}} \right] dp \tag{4}$$

Instead of solving this expression generally, we will consider two limiting cases for the pressure.

Case I: Non-Relativistic Degenerate Gas: Here $p_0 \ll m_e c$ and so

$$\left(1 + \frac{p^2}{m_e^2 c^2} \right) \to 1$$

Therefore, our above expression (3) becomes

$$P = \frac{8\pi}{3h^3 m_e} \int_0^{p_0} p^4 dp = \frac{8\pi p_0^5}{15h^3 m_e}$$

To get an expression for p_0 in terms of electron number, realise that the electron density per unit volume is defined as

$$n_e = \frac{N}{V} = \frac{8\pi p_0^3}{3h^3}$$

where we have used (2) again. Rearranging this gives our desired expression for the critical pressure value

$$p_0 = \frac{h}{2} \left(\frac{3n_e}{\pi} \right)^{\frac{1}{3}}$$

Putting this back in to our expression for pressure in this case gives the end result of

$$P = \frac{h^2}{20 m_e} \left(\frac{3}{\pi} \right)^{2/3} n_e^{5/3}$$

Case II: Relativistic Degenerate Gas: In this case, $p_0 \gg m_e c$ and the velocity v is apporaching the speed of light c. Hence,

$$\left(1 + \frac{p^2}{m_e^2 c^2} \right) \to \left(\frac{p}{m_e c} \right)^{-1}$$

Thus, in this situation (3) becomes

$$P = \frac{8\pi c}{3h^3} \int_0^{p_0} p^3 dp = \frac{8\pi c p_0^4}{12h^3}$$

We can use the same expression for p_0 as in Case I to get our expression for pressure as

$$P = \frac{hc}{8} \left(\frac{3}{\pi} \right)^{1/3} n_e^{4/3}$$

We have now derived an expression for the pressure of a degenerate gas. From this, we will be able to derive our desired equations of state for degenerate star.
In a fully ionised gas, the number of electrons per unit volume is given by

$$n_e = \left(\frac{\#\text{electrons}}{\text{nucleon}}\right)\left(\frac{\#\text{nucleons}}{\text{volume}}\right) = \left(\frac{Z}{A}\right)\frac{\rho_m}{m_H}$$

where Z corresponds to the number of protons, A the number of nucleons and m_H the mass of hydrogen atom. Using this, the pressure above can instead by represented as

$$P = \frac{(3\pi^2)^{2/3}}{5}\frac{\hbar^2}{m_e}\left[\left(\frac{Z}{A}\right)\frac{\rho}{m_H}\right]^{5/3}$$

which gives us the equation of state in the polytropic form described at the start of this section. Namely,

$$P = K_1\rho^{\frac{5}{3}}$$

where the value of n is 1.5. We do the exact same thing for relativistic case in order to get

$$P = K_2\rho^{\frac{4}{3}}$$

where here the value of n is 3 instead.

2.1.2 What does this equation of state mean for white dwarfs?

From these expressions we can make numerous enlightening observations. Firstly, notice that the pressure of a white dwarf is independent of its temperature.
Secondly, we are able to derive a relation between the mass of a white dwarf and its volume. We set the central pressure of the star to the (non-relativistic) degeneracy pressure in order to get

$$\frac{2}{3}\pi G\rho^2 R^2 = \frac{(3\pi^2)^{2/3}}{5}\frac{\hbar^2}{m_e}\left[\left(\frac{Z}{A}\right)\frac{\rho}{m_H}\right]^{5/3}$$

Then, by assuming a constant density of

$$\rho = \frac{M_{WD}}{\frac{4}{3}\pi R_{WD^3}}$$

and substituting in we get the expression

$$MR_{WD}^3 = \left[\frac{(8\pi)^{2/3}}{10}\frac{G}{m_e}\left[\left(\frac{Z}{A}\right)\frac{1}{m_H}\right]^{5/3}\right]^3 = A$$

where A is a constant. Hence, the mass of the white dwarf is inversely proportional to its radius. Simply put, *the more massive a white dwarf is, the smaller it will be*.

Finally, we can determine the Chandrasekhar mass that was previously discussed. Recall that this is the most massive a white dwarf can become. To derive this, we set the

central pressure to the degeneracy pressure again, but this time we use the expression for *relativistic* degeneracy pressure as the most massive white dwarfs will be supported by this type. This yields the following expression

$$\frac{2}{3}\pi G\rho^2 R^2 = \frac{(3\pi^2)^{1/3}}{4}\hbar^2 c\left[\left(\frac{Z}{A}\right)\frac{\rho}{m_H}\right]^{4/3}$$

If we again assume constant density then by substituting and rearranging we get

$$M_{CH} \approx \frac{3\sqrt{2\pi}}{8}\left(\frac{\hbar c}{G}\right)^{3/2}\left[\left(\frac{Z}{A}\right)\frac{1}{m_H}\right]^2 \approx 1.4M_\odot$$

which matches was what stated previously.

2.2 Properties of White Dwarfs and Neutron Stars

Object	Mass (in solar masses)	Radius (m)	Density (g/cm^3)	Temperature within a few thousand years of formation (K)
Earth	$3\text{x}10^{-6}$	$6.4\text{x}10^6$	5	$T_{core} \sim 4\text{x}10^3$ - $7\text{x}10^3$ $T_{surface} \sim 300$
Sun	1	$1.5\text{x}10^8$	1.4 (average) ~160 (core)	$T_{core} \sim 15\text{x}10^6$ $T_{surface} \sim 6000$
White dwarf	$0.07 \leq M_{WD} < 1.4$ Typically ~ 0.6	Typically $\sim 10^7$ ($\sim R_{Earth}$)	Typically ~ 10^6	$T_{core} \sim 10^7$ $T_{surface} \sim 8000 - 40{,}000$ typically (cools down over time)
Neutron star	$1.4 \leq M_{WD} < 3$ Typically 1.4	$10^4 \leq R_{NS} \leq 1.5\text{x}10^4$ (~ size of a city)	~ $7\text{x}10^{14}$	$T_{core} \sim 10^{10}$? (unknown) $T_{surface} \sim 10^6$-10^8 (cools down over time)

Figure 11: Table of Compact Object Properties

We utilise this section to outline some of the key properties about white dwarfs and neutrons stars, summarising what we have described and derived so far.

2.2.1 White Dwarfs

- Consist of a plasma of nuclei (including helium, carbon, oxygen, sodium, magnesium etc.) and degenerate electrons.
- There is *no* fusion occurring.
- MR_{WD}^3 is constant, and so, the more massive a white dwarf is the smaller it will be.
- The luminosity of a white dwarf is given by the Stefan-Boltzmann Law:

  $$L = 4\pi\sigma R^2 T^4$$

  and ranges from $2 \times 10^{-3}\,\text{L}_\odot$ to $1 \times 10^{-1}\,\text{L}_\odot$.

- The cooling timescale is between 10^8 and 10^9 years.
- The peak emission wavelength is given by Wien's displacement law:

$$\lambda_{\text{peak}} T = 2.898 \times 10^{-3}\,\text{m K}$$

For a 10 000 K white dwarf, peak $\lambda \sim 300\,\text{nm}$ which is in the ultraviolet part of the electromagnetic spectrum.

2.2.2 Neutron Stars

- These objects are almost entirely comprised of neutrons (formed from the combination of electrons and protons). They are supported by neutron degeneracy pressure and the strong nuclear force.
- Like for white dwarfs, there is *no* fusion occurring. These objects cool over time.
- There is a limit to the mass of a neutron star, analagous to the Chandrasekhar mass for white dwarfs. This is called the **Tolman-Oppenheimer-Volkoff limit** and simulations show it to be $\sim 2-3M_\odot$.
- The equation of state of a neutron star is not well understood[4] as its density is greater than that of a nucleus.
- Neutron stars take a few hundred years to cool down to $10^6\,\text{K}$ and then a further 10^7 years to cool to the order of thousands of kelvin.
- For a neutron star with a temperature of $10^6\,\text{K}$, its peak wavelength would be 2.9 nm (again derived from Wien's law) which is in the X-ray part of the electromagnetic spectrum.

2.3 Properties and Physics of Black Holes

We begin this subsection with the statement of the **No Hair Theorem**. This theorem states that an **isolated, stationary** black hole can be completely characterised by **three** externally observable properties. These properties are the **mass, angular momentum** or (**spin**) and **electric charge**. This means that no matter what a black hole absorbs other time or how it is created, only the three properties stated can distinguish one from another. Any other information that falls into the black holes is lost.

2.3.1 Characterisations and Properties

We consider each of the properties that can define a black hole (as given by the above No Hair Theorem) in turn.
Mass: Black holes are in one of the following three categories depending on their mass.

- Those between three and a few hundred solar masses are called **stellar-mass black holes**
- Those between a few hundred solar masses and $10^5 M_\odot$ are called **intermediate mass black holes**

[4] Understanding the mechanisms of the cores of neutron stars is an active area of research.

- Those between $10^6 M_\odot$ and $10^9 M_\odot$, such as the ones found in the centres of galaxies, are called **supermassive black holes**

Of the above, only stellar mass black holes can be formed by the collapse of stars in the way we outlined previously. More massive black holes are created by accreting matter or by merging with other black holes. This will be covered more later in the course.
Angular Momentum: Overall, the angular momentum of black holes is high. They are observed to rotate at 90% of the speed of light just outside the Schwarzschild radius (which will be defined properly soon). This high angular momentum is due to the fact that the star which becomes a black hole has angular momentum and so when its core collapses to a smaller radii, it is required to spin faster for angular momentum to be conserved.
Electric Charge: In summary, black holes have a low electric charge. Highly charged black holes are not expected to form as in highly charged cores of stars, electrostatic repulsion would be helping to fight gravitational collapse. In addition to these characterisations, black holes are also classified with reference to their properties as follows:

- **Kerr Black Holes** are *spinning* and *uncharged*. These are the most common type of black holes.
- **Schwarzschild Black Holes** are *non-spinning* and *uncharged*.
- **Reissner-Nordstrom Black Holes** are *non-spinning* and *charged*.
- **Kerr-Newmann Black Holes** are *spinning* and *charged*

In addition to the elements included in the No-Hair theorem, we can also discuss the 'size' of black holes. The black hole itself is a **singularity** with an infinitely small radius and infinitely high density. Around this, space-time is infinitely curved and the laws of physics as we experience and are familiar with begin to break down.

When we discuss the 'size' of a black hole, we are usually referring to the **Schwarzschild radius** which is defined as the radius within which nothing, not even light, can escape the black hole singularity. Everything at a radii smaller than this is obscured to us but note that this is *not* a physical barrier. The **event horizon** is a spherical 'surface' that encompasses the black hole at the Schwarzschild radius, but note once more that this is still not a physical entity. To do a formal derivation of the Schwarzschild radius, general relativity is required. Here, we do a Newtonian approximation of said derivation to get a rough idea of the size of this measurement. For a test particle of mass m at a radius R to escape a body of mass M, its kinetic energy must be at least equal to its potential energy. Thus,

$$\frac{GMm}{R} = \frac{1}{2}mv_{\text{esc}}^2$$

where v_{esc} refers to the escape velocity of the test particle. At the Schwarzschild radius, only light can escape and thus $v_{\text{esc}} = c$. Substituting this in and rearranging for R gives

$$R_{\text{sch}} = \frac{2GM}{c^2}$$

2.3.2 Effects of Black Holes on surroundings

According to general relativity, an object with mass bends space-time. Objects moving past these objects will have to follow this curvature of space-time and this includes massless particles such as light. This leads to idea of a **photon capture radius** around a black hole. Recall the definition of the *impact parameter*, b, which is the distance of closest approach between two objects. Observe the diagram below - there are three

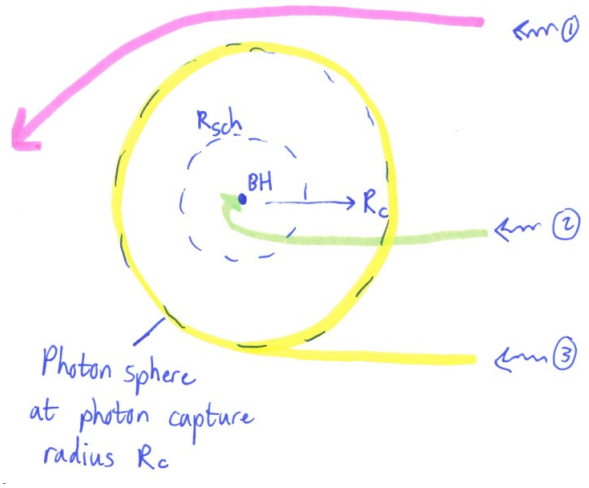

Figure 12: Diagram of possible interceptions of a photon with a black hole

possible cases depending on the impact paramter.

- **Case 1:** When a photon approaches with $b > R_c$, its path is bent around the black hole but the photon is not captured.
- **Case 2:** When a photon appraoches with $b < R_c$, it is captured and so is not observable.
- **Case 3:** When a photon approaches with $b = R_c$, it will be captured onto an unstable orbit around the black hole.

This last case demonstrates what we mean when we say *photon capture radius*, which is the distance from the black hole where gravity is so strong that the photons are forced to orbit the black hole. This radius is given by

$$R_c = \frac{3GM}{c^2}$$

There is key distinction with this concept and the Schwarzschild radius - something with at a radius *less* than the Schwarzschild radius can *never* escape the black hole. In contrast, something at a radius above the Schwarzschild radius but below or equal to the photon capture radius could still accelerate away from the black hole or be disturbed into spiralling down into it. This last possibility is why the photon capture radius is sometime referred to as the **last photon orbit**.

2.3.3 General Notes

We have seen in this section that gravity can be treated as the curvature of space-time and that the path of light is bent around massive objects. It should also be noted that time itself slows down in curved space-time and that, for rotating black holes, **relativistic frame-dragging** occurs near their Schwarzschild radius. This is where space-time is 'dragged' in the direction of the spin and all objects in this region are forced to move in the same direction of rotation.

3 Radiation Processes

3.1 Overview of processes relevant to compact objects

For main sequence stellar objects, blackbody curves provide a fairly accurate description of their emission spectra. In comparison, the high energy environments around compact objects as well as the *interactions* of these objects with said surrounding environment leads to other important processes occurring. In this subsection we will proceed with a quick discussion of some of these processes and how together they give a more coherent picture of what is occurring.

3.1.1 Blackbody Radiation

Nevertheless, the first concept we are required to consider is the **thermal blackbody** or **Planck radiation**. Recall that the Planck function is given by

$$B_\lambda(T) = \frac{2hc^2}{\lambda^5}\left[\frac{1}{e^{\frac{hc}{\lambda kT}}-1}\right]$$

which describes a general emission spectra of the medium assumed to be acting as a blackbody. But note that this depends on an intrinsic property of said medium, namely its temperature. To get the total emission of the medium as a blackbody, we integrate over all wavelengths as such

$$B(T) = \int_0^\infty B_\lambda(T)d\lambda = \frac{\sigma T^4}{\pi}$$

where σ is the Stefan-Boltzmann constant. On the other hand, differentiating the Planck function and setting this to zero in order to find a critical point gives

$$\frac{dB_\lambda(T)}{d\lambda} = 0 \implies \lambda_{\max} T = 2.898 \times 10^{-3}\,\mathrm{mK}$$

which is an expression known as **Wien's Law**. Recall that we can calculate the total luminosity of an object with the following expression

$$L = 4\pi R^2 \sigma T$$

What temperature is being considered here? As stated in the introduction to this section, stars behave generally behave like a blackbody with an *effective temperature* T_{eff} corresponding to a blackbody that emits the same total power as the star being considered (per unit area).

3.1.2 Thermal Bremsstrahlung (Braking Radiation)

This is a *high energy* phenomenon, occurring in stars with a peak wavelength in the X-ray section of the electromagnetic spectrum. As an incoming electron from the surrounding medium is deflected by a charged proton or ion, a photon is produced from the sudden deceleration of said photon. The energy of the photon produced is given by

$$E_\gamma = h\nu = \frac{1}{2}m_e\left(v_2^2 - v_1^2\right)$$

and so, since the velocity can have a range of values, a continuous spectrum is produced.

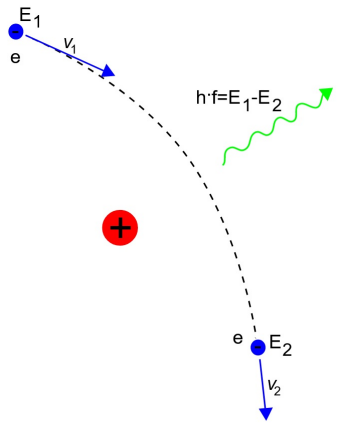

Figure 13: Diagram of the Bremsstrahlung process

3.1.3 Cyclotron Radiation

This phenomenon occurs when a non-relativistic (i.e. $v \ll c$) free electron is deflected by a magnetic field. The resulting circular motion leads to an acceleration of the electron which in turn causes an emission of radiation in the form of a photon. Recall that the deflection of the electron is a result of the Lorentz force, given by

$$F = m_e a = e\mathbf{v} \times \mathbf{B}$$

where the circular motion is perpendicular to the direction of the magnetic field. Moreover, the centripetal ('centrifugal') force is given by

$$F = \frac{m_e v^2}{r} = evB$$

which means that the expression for angular frequency is given by

$$\omega = \frac{eB}{m_e} = \frac{v}{r}$$

Recall that rotational frequency is given by

$$\nu = \frac{\omega}{2\pi}$$

and so, altogether, this gives the following expression for the **fundamental cyclotron frequency**

$$\nu_e = \frac{eB}{2\pi m_e}$$

When considering the environment around a stellar object, there is a distribution of velocities for the surrounding electrons moving along the field lines. This cannot be solved analytically and so a numerical solution is required. But when calculated this results in the frequency of the emitted cyclotron photons being integer multiples of the above fundamental cyclotron frequency, hence the name.

When the electrons approach 'mildly' relativistic speeds, **cyclotron beaming** occurs where the emission of the photons is beamed in the direction of motion of the electron (i.e. perpendicular to the direction of the magnetic field lines). This beaming is stronger in the higher harmonics. The diagram below demonstrates the intensity of emission observed at different wavelengths and different angles of observation From this, it is

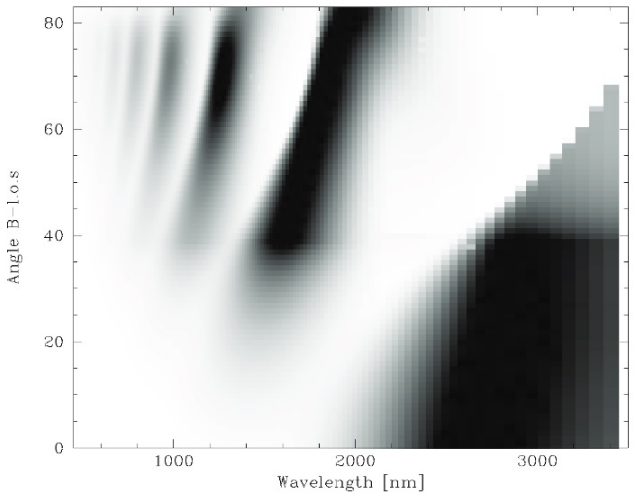

Figure 14: Intensity distribution of cyclotron emission

clear that both the wavelength and angle of viewing chosen will have a noticeable impact on the amount of cyclotron emission observed.

3.1.4 Synchotron Emission

The last high energy effect we will discuss is **synchotron emission**, which is electromagnetic radiation that is emitted from highly relativistic (i.e. $v \sim c$) electrons in a magentic field. This occurs once again since the spiralling motion, due to the force from the magnetic field, constitutes an acceleration and accelerating charges emit photons. Since the electron is moving at relativistic speeds, the radiation is particularly intense and the harmonics merge into a continuum. Furthermore, the emission is heavily beamed in the direction of travel of the radiating electron.

3.1.5 Scattering

The final type of important radiation interactions we will discuss are the scattering processes in the specific case of *ionised plasmas*.

The first of these is **Thompson scattering**, which occurs when a relatively low energy photon elastically scatters off of an electron. This means that the incoming energy E_γ and outgoing energy $E_{\gamma'}$ of the photon is equal. The probability or *cross-section* for this interaction is given by the Thompson cross section coefficient, which has a value of $\sigma_T = 6.65 \times 10^{-25}\,\mathrm{m}^2$.

The next type of scattering event is **Compton scattering**, which occurs when a high energy photon scatters off an electron, transferring a considerable amount of its momentum to the electron, with the remainder carried off by the final photon. The change

in wavelength of the photon is then given by the expression

$$\lambda' - \lambda = \frac{h}{m_e c}(1 - \cos(\theta))$$

where θ is the angle between the initial path of the photon and the final path.

Lastly, there is the process referred to as **inverse Compton scattering** which, as the name implies, is where a high energy electron interacts with a photon and boosts it to a higher energy level.

4 Observational Astronomy

In this section, we will discuss and consider a handful of the methods that astronomers use to identify and evaluate objects that they find within the universe.

4.1 Important Definitions

To begin, we will recall some key definitions and expressions from previous astronomy modules (namely PX144/158 and PX282) that we will utilise to quantify aspects of the objects that are observed.

The first of these is the notion of **magnitudes**, which is a logarithmic system. We calculate the **apparent magnitude** with the following expression

$$m_1 - m_2 = -2.5 \log_{10} \left(\frac{f_1}{f_2} \right)$$

where m_1 and m_2 are the apparent magnitudes of star 1 and star 2 respectively and f_1 and f_2 correspond to the flux of these stars.

We can also calculate the **absolute magnitude** of an astrophysical object, which is what the magnitude of the object would be at 10 parsecs. We calculate this using the **distance modulus**, which has the form

$$m - M = 5 \log_{10} \left(\frac{d}{10\text{pc}} \right)$$

Recall that we can calculate the distance to an astrophysical object in parsecs, with the expression

$$d[\text{pc}] = \frac{1}{\theta(\text{arcsec})}$$

where θ is measuring the parallax of the object in the sky.

4.2 The Electromagnetic Spectrum and Radiation

This subsection is simply a quick recap of the electromagnetic spectrum (EM) and its importance within the astrophysical world. Recall that the EM spectrum has the form in Figure [15] below. Photons are emitted from astrophysical objects across the cosmos, across the entire range of the EM spectrum and form the primary source of our knowledge about the universe.

Of particular importance in this course, is that compact objects like white dwarfs, neutron stars and black holes, when in binaries, emit EM radiation across the *whole* of the spectrum.

It is important to note that the atmosphere of the Earth is opaque to most photons, as figure [16] demonstrates. Thus, observations from space or with advanced adaptive optics from the ground are required to detect the vast amount of photons being emitted from astrophysical objects.

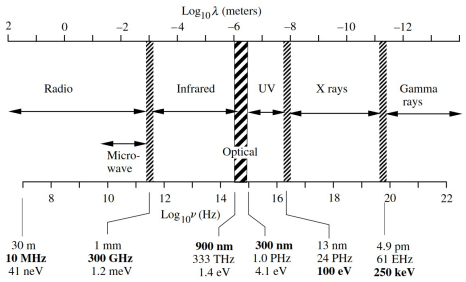

Figure 15: The Electromagnetic Spectrum and its approximate bounds (Credits: Hale Bradt)

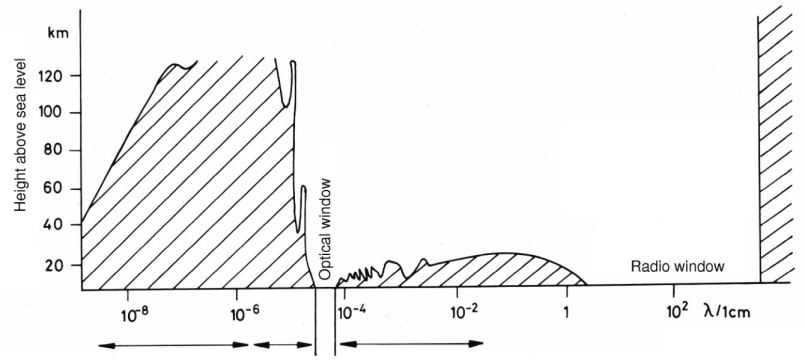

Figure 16: Opacity of the atmosphere of the Earth to different wavelength photons

4.3 Spatial Resolution

The purpose of this section is to serve as a reminder of how astronomers adapt to resolve images in the sky and overcome the difficulties ingrained within telescopic measurements.

4.3.1 Telescopes as Single Slits

To begin, recall the double slit experiment which involves light approaching two slits in a wall which are separated by a distance d. Light is a wave and so interferes as such, thus, when $d\sin(\theta) = n\lambda$ (where n is an integer), constructive interference occurs and when $d\sin(\theta) = \left(n - \frac{1}{2}\right)\lambda$ then destructive interference occurs. This is illustrated in the diagram below: More relevant to us is interference from a single slit, referred to as **Fraunhofer diffraction**. As the plane wave approaches the slit, Huygen's principle tells us that the wave can interfere with itself as it passes through the slit, causing constructive or destructive interference depending on the angle. The reason this is of note to us, is that a single slit experiment is analagous to a telescope, which can be considered equivalent to a circular aperture.

Consider a plane wave approaching this circular aperture of size a. Then it can be shown that the minimum resolution possible for this aperture is given by

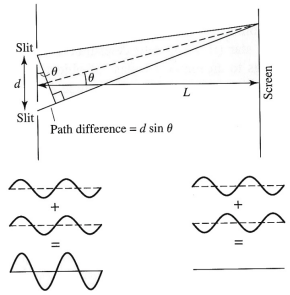

Figure 17: Double Slit Experiment

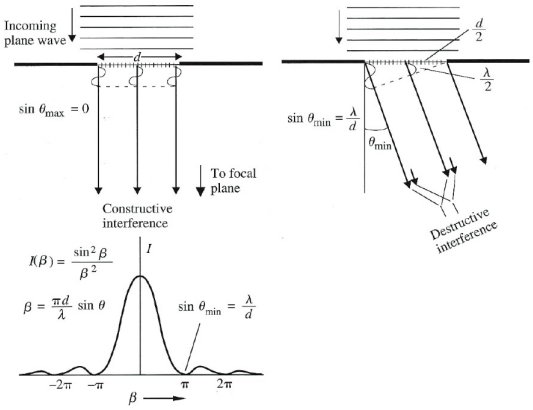

Figure 18: Single Slit Interference

$$\theta_{\text{min}} = 1.22\frac{\lambda}{a}$$

From this, we can tell that a better resolution will be given by observing at shorter wavelengths and with bigger apertures. In reality however, for ground based telescopes **atmospheric turbulence** prevents one from reaching the diffraction limit. Thus, it is usually this which limits the resolution.

4.3.2 Atmospheric Seeing

The atmosphere can be modelled as containing layers of turbulent cells that perturb the incoming light from space. This is shown diagramatically below. The 'speckles' in the image denote the interference pattern of several individual images.

There are several ways to negate atmospheric seeing. If the telescope is on Earth, it can be built in a favourable location with smooth laminar flows of air such as on top of mountain. The telescope can then include adaptive optics, which effectively repair the wavefront by changing the shape of the mirror. Alternatively, the telescope can be placed in space to avoid the atmosphere altogehter, but this of course presents its own challenges such as more complicated logistics.

One final thing to note is how we measure things on the sky, and this is the concept

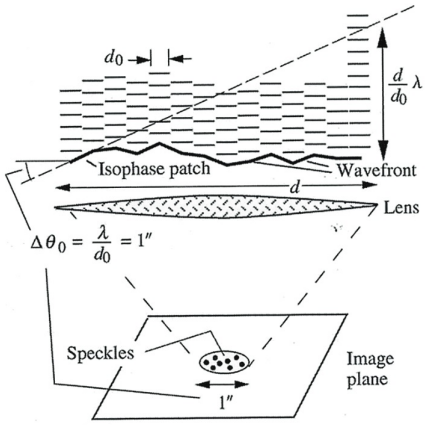

Figure 19: Atmospheric Turbulence

of the **angular radius** or **distance**, which is given by

$$\alpha = \frac{R}{d}$$

where R is the spatial extend of the astrophysical object and d is the distance to the object. From this, we can calculate the minimum separation of two objects that a telescope is able to resolve.

4.4 Information from Photons

The final part of this section is dedicated to discussing what kind of information we can obtain from photons (or, equivalently, imaging and spectroscopy).

4.4.1 Imaging

From direct imaging, there are several things one can determine about the astrophysical object being considered. These include:

- **Morphology:** If the images are able to be adequately resolved, then the overall structure and shape of the object can be ascertained.
- **Position:** The location of the object can be deduced from sharp images.
- **Proper Motion:** Taking many images over a considerable amount of time allow one to deduce the motion of the object(s) being considered.
- **Colours:** Using different filters on a telescope enables one to identify the colours of particular objects, which allows for the temperature to being reasonably approximated.
- **Variability:** Taking many images over timescales ranging from less than a second to years can allows for the consideration of how an object is chaning over time.

4.4.2 Spectroscopy

This was historically an expensive and delicate technique, as only one observation of a specific object at a time was possible. Modern spectroscopes are capable of viewing 500 to 5000 at any one time, but they are required to be relatively nearby.

Spectroscopy is of particualr importance as it allows astronomers to deduce a lot of the 'hidden' physics of the objects being observed. Thus, interpreting spectroscopy usually requires the use of **models**, but the spectroscopy can also inform the models as well. There are four main things that can be deduced from spectroscopy. These are

- **Temperature and Chemical Abundance:** The conditions the star is existing in can be deduced by looking at the absorption and emission lines and correlating them with the known wavelengths of specific chemical elements/ions and compounds.
- **Magnetic Fields:** The magnetic fields can be deduced from the Zeeman splitting of absorption lines. This usually requires quite a strong magnetic field being present around the object.
- **Radial Velocities:** These can be deduced from plotting so-called 'Rainfall' diagrams, which are time series of the spectra of an astrophysical object, and utilising the Doppler effect with what the wavelength is known to be to deduce the velocity of the system.
- **Redshift:** This can be deduced by comparing the emission lines being observed and comparing them to what the values are known to be.
- **Other Material:** Also from the measurement of spectra, the noise that is present before the actual measurement of an object (such as the Lyman-α forest example in the notes) can give some indication of the material that is present between the object and the observer.

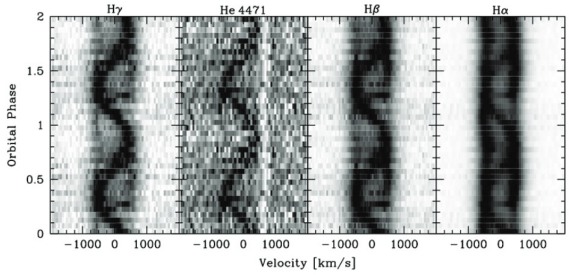

Figure 20: Example of a Rainfall Diagram

5 Binary Stars

We now turn our attention to **binary star systems**, which are systems of two stars that orbit one another. These are of great importance to astrophysics as they provide fascinating examples of stellar evolution, allow astrophysicists to analyse and deduce much more about a system than may be possible for lone stars. Furthermore, binary systems are able, in some cases, to facilitating stages in stellar evolution that single stars are not able to reach as we will see.

5.1 The Roche Model

5.1.1 Introduction and Lagrangian Points

To begin with, we must find a way of describing the geometry and equipotential surfaces within these systems in order to understand how material will move around them. This leads to us to a model called the **Roche model** or **Roche potential**, derived by Édouard Roche and Joseph-Louis Lagrange in the 19th century.

Consider a binary system and assume that the stars are point masses that orbit in the $x-y$ plane. This is illustrated in the diagram below:

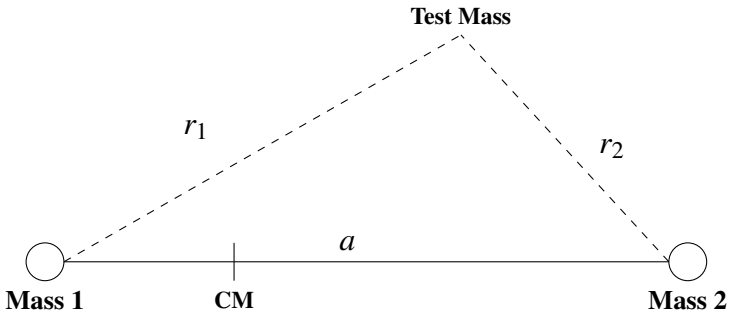

Figure 21: 2D Binary System Visualisation

where *CM* denotes the centre of mass and a is the *binary separation*. Let

$$q = \frac{M_2}{M_1}$$

denote the **mass ratio** and

$$\omega = \frac{2\pi}{P}$$

denote the angular frequency. The x-coordinate position of the centre of mass is given by

$$x_{CM} = \frac{M_2}{M_1 + M_2} = \frac{q}{1+q}$$

and the **Roche potential**, denoted by ϕ_r, is given by

$$\phi_r = \underbrace{-\frac{GM_1}{r_1}}_{\text{Due to Star 1}} - \underbrace{\frac{GM_2}{r_2}}_{\text{Due to Star 2}} \underbrace{-\frac{1}{2}\omega^2\left((x-x_{CM})^2+y^2\right)}_{\text{Centripetal Force}}$$

If we set $\phi_r = 0$, we get a solution that is represented by the surface below. For a more

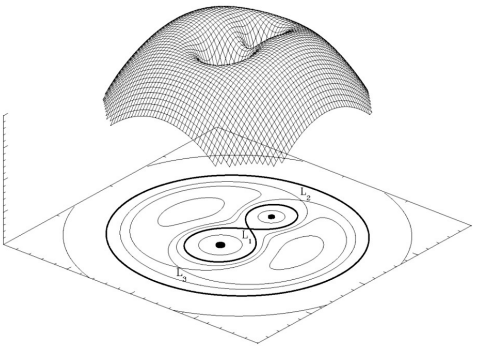

Figure 22: Roche Potential 3D Geometry

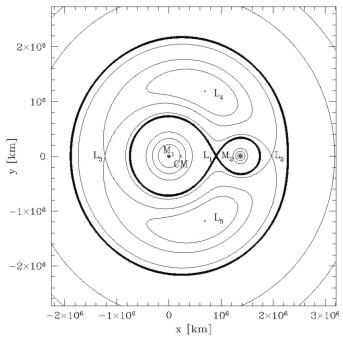

Figure 23: 2D Plot of Roche Poential Lines

specific example, if we take $q = 0.2$ and the period of the orbit, P, to be 7 hours then we get a two dimensional plot of the x and y position as follows On the figure (although this is applicable to any two-body system), the L_i points denote the **Lagrangian points**, which are points of zero-potential for small-mass objects which are under the influence of gravity from the two larger bodies creating the Roche geometry. L_1, L_2 and L_3 are *unstable* positons of equilibrium, meaning that a deviation in position from them will cause any object orbiting at them to fall out of orbit. In contrast, L_4 and L_5 are *stable* points of equilibrium as they are **potential wells**.

Of particular importance to the systems we will be discussing, one can observe that if the M_2 star expanded, then it would take on the shape of its Roche lobe (which is not perfectly spherical). Furthermore, if M_2 began to fill its Roche lobe the point L_1, which is called the **inner Lagrangian point**, would be the **natural point of mass transfer**. Note that if M_2 did in fact fill its Roche lobe, then it would not be able to grow any more as any material from this point onward would be filtered onto the M_1 star. Thus, the size of the Roche lobe is the *maximum size* M_2 can grow.

Another point of note is L_2, which in this model is the point at which material is **most easily ejected**.

The shape of the Roche lobes depends on the mass ratio q and the absolute dimensions, or size, can be determined from Kepler's third law. This is the subject of the next subsection.

5.1.2 Important Definitions and Equations

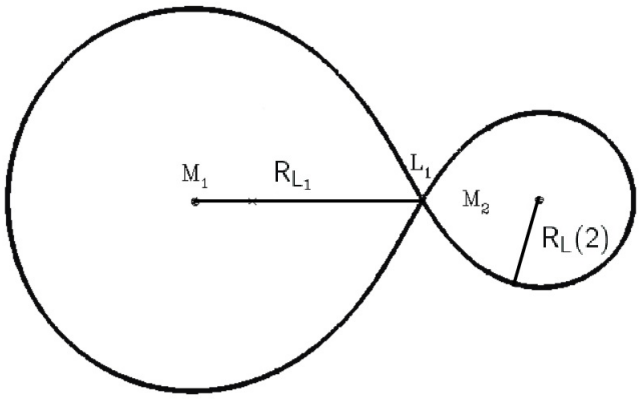

Figure 24: Roche Lobes

Here we assume without loss of generality that star one has a higher mass than star two, i.e. $M_1 > M_2$. As usual, let a denote the orbital separation of star one and star two. The distance from star one to the inner Lagrangian point L_1 is given by

$$\frac{R_{L_1}}{a} = \begin{cases} (1.0015 + q^{0.4056})^{-1} & \text{for} \quad 0.04 \leqslant q \leqslant 1 \\ 0.5 - 0.227\log(q) & \text{for} \quad 0.1 \leqslant q \leqslant 10 \end{cases}$$

As discussed previously, the Roche lobe that star two will fill is not perfectly spherical. Instead we refer to $R_L(2)$ as being the **volume equivalent radius** of the secondary star Roche lobe. This value is given by the expression

$$\frac{R_L(2)}{a} = \frac{0.49q^{2/3}}{0.6q^{2/3} + \ln(1+q^{1/3})}$$

We will refer to the object which had the more massive (main-sequence) star as being the **primary** and the less massive star being the **secondary**. Note that usually, having a more massive main sequence star would mean it is brighter but this is **not** the case for binaries involving white dwarfs, neutron stars and of course black holes.

5.2 Binary System Configurations

5.2.1 Types of Binary System

In this subsection, we are going to consider different types of binary systems as well as the evolution of their Roche lobes. The three possible configurations are shown diagramatically below: It is important to note that in all of these, we are once again assuming that $M_1 > M_2$ or that the mass ratio $q < 1$.

On the **left**, we have what is referred to as a **detached system** where a secondary has expanded but does not fill its Roche lobe. These systems are very typical of white dwarfs, neutron stars and black holes. A specific example of these is a *post common envelope system*.

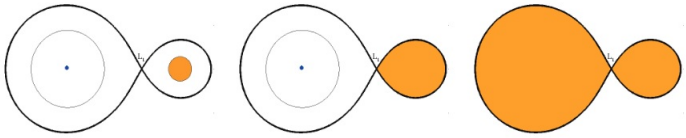

Figure 25: Different types of Binary System

The **middle** arrangement is called a **semi-detached system** where a secondary *has* filled its Roche lobe. In this arrangement, mass transfer occurs at the L_1 Lagrangian point. The most common examples of these kinds of systems are **cataclysmic white dwarf binaries**, where the smaller star transfers mass to the white dwarf resulting in a detonation event.

On the right is a system called a **contact binary**. These systems are very distinctive when observed, as their light curves are continuously varying. This class of binaries are called Algols and they have a period of days.

5.2.2 Criteria for Roche Lobe Overflow

We now seek to quantify when this mass transfer may occur or, in other words, when an object in a system will fill its Roche lobe. This can be derived from Kepler's third law and the formula given previously for $R_L(2)$, where it can be calculated that the average density of the star is given by

$$\overline{\rho} = \frac{M_2}{\frac{4}{3}\pi R_L^3(2)} = 1.07 \times 10^5 P^{-2} \quad \text{for} \quad 0.01 < q < 1$$

where the units have been chosen so that the period P is given in *hours*. Rearranging this, we can thus tell that an object of a given size will fill its Roche lobe at

$$P = \sqrt{\frac{1.07 \times 10^5}{\overline{\rho}}}$$

where, to be clear, this time is again given in hours. Hence, note that the time taken for the Roche lobe to be filled *only* depends on the (average) density of the star.

5.3 Interactions of Binary Systems

Now that we know the different types of binary systems we want to consider how the two astrophysical objects interact with one another and how this affects our observation of the system.

5.3.1 Ellipsoidal Variations

Consider the following arrangement (recall that this is an example of a semi-detached system): When looking what is in the plane of the page up and down, one would see the most light as neither object is being obscured by the other. In contrast, looking left or right in the plane of the page would lead to a reduction in light as one object blocks the other for some time. This means that in one phase (where the length can be calculated from the radial velccity) one would expect to see two maxima and two minima, resulting in a **two-humped curve**. An example of this type of curve is given

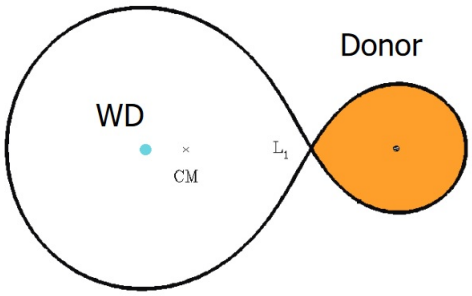

Figure 26: Semi-Detached System

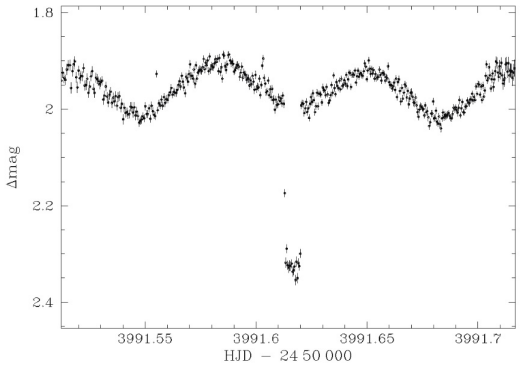

Figure 27: Example of Ellipsoidal Variations

below. Notice that in each phase there is a primary phase, where the donor eclipses the white dwarf and a much shallower secondary phase where the white dwarf instead eclipses the donor star.

5.3.2 Reflection or Irradiation Effect

This is a similar situtaion to the ellipsoidal variations, in that we are still considering a semi-detached system, but in this instance we are considering a donor with one half being much hotter than the other half due to the heat being transferred from a very hot white dwarf companion. This is illustrated in the diagram below. Here, the left half

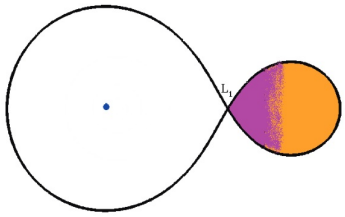

Figure 28: Irradiation Illustration

of the donor, which is shaded purple, is considerably hotter than the orange right half. Thus, the system will look brightest when observed from what is the right direction in

the plane of the page. Thus, per orbital cycle, there is one maximum and one minimum in contrast to the two of the ellipsoidal variations.

5.4 Characteristic Timescales of Stars

This subsection is seemingly a quick aside, but is of significant importance for understanding specific scenarios of a star. In general, a timescale is defined as a property of a system divided by the rate of change of said property. They provide an order of magnitude estimate for how long a particular process will take.

There are three key timescales for stars, the first of which is the **dynamical** or **free-fall timescale**, denoted τ_{Dyn}. This is the timescale on which a star will adjust back to hydrostatic equilibrium after being perturbed from it (via expansion or contraction). It can be calculated as follows

$$\tau_{\text{Dyn}} = \frac{R}{\dot{R}} = \frac{R}{v_{\text{esc}}} = \frac{R}{\sqrt{\frac{2GM}{R}}} = \sqrt{\frac{R^3}{GM}}$$

But since R^3 is proportional to volume, we are able to write this as

$$\tau_{\text{Dyn}} \approx \frac{1}{\sqrt{G\bar{\rho}}}$$

where $\bar{\rho}$ denotes the *mean density* of the star in question. As a specific example, the dynamical timescale of the Sun is approximately 1000 seconds. Solar oscillations are seen on these timescales.

The second of the key timescales is the **Kelvin-Helmholtz** or **thermal timescale**, denoted τ_{KH}. This is the timescale on which a star will adjust its thermal structure or, in particular, on which it will regulate the rate of fusion in order to maintain equilibrium. Here, we consider thermal energy divided by its rate of change i.e. the luminosity of the star

$$\tau_{\text{KH}} = \frac{E}{\dot{E}} = \frac{E_{\text{TH}}}{L} = \frac{E_{\text{P}}}{2L}$$

where E_P denotes the potential energy of the star and the last equality arises from the Virial theorem. When considering a star, the potential energy being considered is *gravitational* potential energy and so, if a uniform density sphere is assumed, we have the following expression

$$E_P \approx -\frac{3GM^2}{5R} \approx \frac{GM^2}{R}$$

Thus, the Kelvin-Helmholtz timescale is given by

$$\tau_{\text{KH}} \approx \frac{GM^2}{RL}$$

Considering the Sun again, the Kelvin-Helmholtz timescale is around 10^7 years. This was the discrepancy that vetoed the idea that stars are powered entirely by the transition of thermal to potential energy.

The final timescale of importance to our considerations is the **nuclear timescale**, denoted τ_{Nuc}. This denotes the timescale on which the chemical composition of the star being considered changes. This is described by the expression

$$\tau_{\text{Nuc}} = \frac{E}{\dot{E}} = \frac{\varepsilon M c^2}{L}$$

where ε denotes the efficiency of the particular fusion process being considered. For example, for the fusion of hydrogen to helium ε is about 0.7%. Thus, for the Sun, the nuclear timescale for the Sun to convert all hydrogen into helium is about 10^{11} years.[5]

5.5 Angular Momentum and Mass Transfer

We now turn our attention to the variation of angular momentum in a binary system that is undergoing mass transfer.

5.5.1 Expression for Angular Momentum

In order to derive an expression for the angular momentum of this system, consider the two masses orbiting their common centre of mass, as depicted in the image below. As usual, let a denote the orbital separation between the two masses and let a_1 and a_2

Figure 29: Binary System (Considered to be moving counter-clockwise)

denote the distance from mass 1 to the centre of mass and mass 2 to the centre of mass respectively. Then we have

$$a_1 = a\frac{M_2}{M} \quad \text{and} \quad a_2 = a\frac{M_1}{M}$$

where $M = M_1 + M_2$ is the total mass of the stars. Note that we are assuming $M_1 > M_2$. The angular frequency of a system is given by

$$\omega = \frac{2\pi}{P} = \frac{v}{r}$$

where P denotes the period, v denotes the orbital velocity and r denotes the radius. Furthermore, Kepler's third law tells us that

$$P^2 = \frac{4\pi^2 a^3}{GM}$$

Substituting this value into the equation for angular frequency gives that

$$\omega^2 = 4\pi^2 \cdot \frac{GM}{4\pi^2 a^3} = \frac{GM}{a^3}$$

Now, recall that the angular momentum of a system, denoted J, is given by

$$J = mvr = m\omega r^2$$

[5]The actual value is 10^{10} years, since not all of the hydrogen gets burned.

Thus, we have that the total angular momentum of the binary system is expressed as

$$J_{\text{tot}} = J_1 + J_2 = (M_1 a_1^2 + M_2 a_2^2)\omega$$

Substituting our expressions for ω, a_1 and a_2 and rearranging then gives that this is equal to

$$J_{\text{tot}} = \left(\frac{M_1 M_2^2}{M} + \frac{M_2 M_1^2}{M}\right)\frac{a^2}{M}\left(\frac{GM}{a^3}\right)^{1/2}$$

Thus, after some reduction we have that

$$J_{\text{tot}} = M_1 M_2 \left(\frac{Ga}{M}\right)^{1/2} = M_1 M_2 \left(\frac{Ga}{M_1 + M_2}\right)^{1/2}$$

5.5.2 Impact on the Binary Separation

We now consider a binary system where the M_2 star has expanded to fill its Roche lobe and is thus transferring mass through the inner Lagrangian point onto the accretor. This is illustrated in the figure below. Here, $\dot{M}$ denotes the **mass transfer rate**. We are

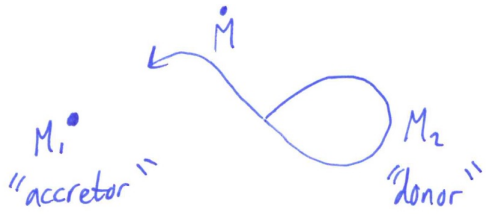

Figure 30: Mass Transfer Situation

considering the situation where the mass transfer is **conservative**, meaning we have the following:

- $\dot{M}_2 < 0$ (i.e. the Donor is *losing* mass)
- $\dot{M}_1 = -\dot{M}_2$ (i.e. the Accretor *gains* the lost mass of the Donor)
- $\dot{M}_1 + \dot{M}_2 = 0 \implies \dot{M} = 0$ (i.e. No mass is lost overall)

We are able to rearrange our previous equation for total angular momentum in the following manner

$$J_{\text{tot}} = M_1 M_2 \left(\frac{Ga}{M}\right)^{1/2} \implies a = \left(\frac{J_{\text{tot}}}{M_1 M_2}\right)^2 \frac{M}{G}$$

By considering the logarithmic derivative[6] of a, we can derive an expression for the rate of change of the separation between the two objects over the initial separation. Namely,

$$\frac{\dot{a}}{a} = \underbrace{\frac{2\dot{J}}{J}}_{=0} - 2\frac{\dot{M}_2}{M_2} - 2\frac{\dot{M}_1}{M_1} = -\frac{2\dot{M}_2}{M_2}\left(1 - \frac{M_2}{M_1}\right)$$

[6] See appendix A for a reminder.

where the last equality is since $\dot{M}_1 = -\dot{M}_2$. Thus, we have the following expression

$$\frac{\dot{a}}{a} = -\frac{2\dot{M}_2}{M_2}\left(1 - \frac{M_2}{M_1}\right) = -\frac{2\dot{M}_2}{M_2}(1-q)$$

The expression $-2\dot{M}_2/M_2$ is always greater than zero, so the binary separation in this situation will **only depend on the mass ratio** q. Thus, we have two cases:

- **Case 1:** When $q < 1$ (i.e. $M_2 < M_1$) then we have $\frac{\dot{a}}{a} > 0$. Thus, the orbit will **expand** if mass is transferred from the lower mass star to the higher mass star.
- **Case 2:** When $q > 1$ (i.e. $M_2 > M_1$) then we have $\frac{\dot{a}}{a} < 0$. Thus the orbit will **shrink** if mass is transferred from the more massive star to the lower mass star.

5.5.3 Impact on the Radius of the Roche Lobe

We now want to deduce what effect mass transfer will have on the Roche lobe radius and how this may affect the evolution of the star. Let us denote the Roche lobe radius as R_2. We have another analytic expression for this, proposed by Paul Eggleton, given by

$$\frac{R_2}{a} = 0.462\left(\frac{M_2}{M}\right)^{1/3} \quad \text{for} \quad 0.1 \leqslant q \leqslant 0.8$$

Utilising logarithmic derivatives once again, we can write this in the following way

$$\frac{\dot{R}_2}{R_2} = \frac{\dot{a}}{a} + \frac{\dot{M}_2}{3M_2}$$

Our boxed expression above for binary separation then tells us that this is equal to

$$\frac{\dot{R}_2}{R_2} = -\frac{2\dot{M}_2}{M}\left(\frac{5}{6} - q\right)$$

Once again, the expression $-2\dot{M}_2/M_2$ is always larger than zero, so the ratio of the masses determines how the Roche lobe will respond to mass transfer. We again have two cases:

- **Case 1:** When $q < 5/6$, the orbital separation will increase, **as will the Roche lobe** of the donor star as a consequence of the mass transfer. But we are still considering the same star, thus the mass transfer will stop. This is called **stable mass transfer**.
- **Case 2:** When $q > 5/6$, the orbital separation will decrease and the mass transfer will cause the Roche lobe to **shrink** Mass transfer will then increase leading to **unstable mass transfer** as it leads to runaway mass loss.

This runaway mass loss process provides a major amount of energy to the system. The next subsection is dedicated to discussing this.

5.5.4 Mass Accretion

We begin with a revision of the gravitational potential energy gained by moving towards a star. Consider a test mass (m) an infinite distance away from an accreting star of mass M_1 and radius R. The acceleration due to gravity of the accretor is given by

$$g = \frac{GM}{r^2}$$

and the gravitational force given by

$$F = mg$$

Work is calculated by force multiplied by distance moved i.e.

$$dE = F\,dr$$

And so the total work to move the test mass from the surface to infinity is given by

$$E = m\int_R^\infty g\,dr = m\int_R^\infty \frac{GM}{r^2}\,dr$$

which gives

$$E = \frac{GMm}{R}$$

This is what we will start with when outlining the typical steps within the accretion process.[7]

To begin with, the material that falls towards the accretor **accelerates** and the gravitational potential energy given by the expression above is converted into kinetic energy, given by

$$E_k = \frac{1}{2}mv^2$$

Some of this kinetic energy is transformed into thermal energy, which has the expression

$$E_{\text{th}} = \frac{3}{2}kT$$

This **heats up** the accreting material. After a time, the material then cools by emitting photons which will have an energy

$$E_\gamma = h\nu$$

This is the point where accretion can be directly imaged and identified. Overall, there is a transition from gravitational potential energy to the emission of photons.

It is important to note that for black holes, we have that

$$E = \frac{GM}{R_{sch}}m \implies E = \frac{1}{2}mc^2$$

where we have substituted the equation found for the Schwarzschild radius. This means that that the energy released from accretion onto a black hole is *independent* of the mass of the black hole.

Process	Energy (J/kg)	Scaling to amount of energy produced fusing H $\rightarrow$ He	Scaling to rest mass energy
Fusion H $\longrightarrow$ He	6.3×10^{14}	1	0.007
Accretion onto a White Dwarf	8.0×10^{12}	0.013	8.9×10^{-5}
Accretion onto a Neutron Star	1.9×10^{16}	30	0.21
Accretion onto a Black Hole	4.5×10^{16}	70	0.5

The table above summarises the different amounts of energy being released for different processes. Note that accretion onto a neutron star and black hole release more energy than fusion. Thus, we expect them (and to some extent white dwarfs) to be very luminous sources of high energy radiation when accretion is present.

The rate of accretion onto an astrophysical object is usually given in $M_\odot$ per year when discussing the type of objects we are considering. We can also calculate the accretion luminosity, which is given by the following expression

$$L_{\text{acc}} = \frac{GM\dot{m}}{R}$$

This has units of joules per second. As an illustrative example, consider accretion onto a neutron star. This will have a luminosity of around $10^{30}\,\text{Js}^{-1}$. We can rearrange the above expression to calculate the accretion rate as follows

$$\dot{m} = \frac{LR}{GM} = 8.4 \times 10^{-10} M_\odot \text{yr}^{-1}$$

This means that a solar-like star could 'feed' this neutron star for around a billion years whilst producing this luminosity. Note that since $q < 1$, this is *stable mass transfer* as well.

This has demonstrated that accretion onto a compact object is a powerful source of energy, resulting in intensely luminous displays. The next natural question is as follows: Can a compact object be continuously supplied with higher rates of accretion to produce higher luminosities? As it turns out, there is a limit. This is the subject of the next section.

5.5.5 Eddington Luminosity/Limit/Accretion Rate

Envision the same scenario as in the previous section, that is, an accretor with mass M and radius R and a test mass m falling onto said accretor. As discussed, when the material falls onto the star it releases kinetic energy, heating up the region. The region (illustrated in yellow in figure [31] below) will then cool by emitting photons that travel in the *opposite* direction of the infalling material. As the photons interact with

[7] These steps are written individually to make the process clearer, but they are all happening continuously.

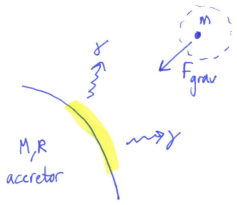

Figure 31: Mass falling onto an accretor

the infalling material, they create a radiation force which transfer momentum to said material. Note that in the plasma surrounding the infalling material (which is assumed to be electrically neutral, fully ionised and pure hydrogen), the protons and electrons are coupled by the Coulomb force as they are oppositely charged. This means they are unable to be separated in this situtation. The electrons then undergo Thomson

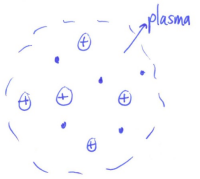

Figure 32: Enhanced image of plasma surrounding the infalling material

scattering with the photons being emitted from the material within the heated region. Considering the forces on the plasma involved, there is a radiation force which acts on the electrons. This has an expression given by

$$F_{\text{rad}} = \frac{\sigma_T F}{c}$$

where σ_T is the Thompson cross section. Inserting this into the luminosity equation gives

$$L = 4\pi R^2 F \implies F_{\text{rad}} = \frac{\sigma_T L}{4\pi R^2 c}$$

The other force at play is the gravitational force, which has the form

$$F_{\text{grav}} = \frac{GMm}{R^2}$$

Since the proton rest mass is so much larger than the rest mass of the electron, we can consider the gravitational force on the electron to be negligible. Thus, the expression for gravitational force is instead

$$F_{\text{grav}} = \frac{GMm_p}{R^2}$$

where m_p denotes the rest mass of the proton.

Now, as an overall system, we have the radiative force pushing the electrons away from the accretor and the gravitational force pulling the protons (mainly) towards it. However, as noted the electrons and protons are coupled by the Coulomb force and

so they drag one another in their respective direction of motion. Thus, overall there is a net force on the plasma which regulates the luminosity able to be produced by the accreting material.

The Eddington luminosity, as it is referred to, occurs when the force of gravity is equal to the radiative force. Setting the expressions above equal to one another and rearranging gives the following expression for this value

$$L_E = \frac{4\pi GMm_p c}{\sigma_T}$$

Note that this value is *independent* of the radius of the accretor.

5.6 Formation of Compact Object Binaries

In this section, we will consider the interaction and eventual fate of certain kinds of binary systems. As was mentioned previously, binary systems are of particular note as they may result in some very intersting systems or final states that single stars would not be able to reach. We will discuss some types of systems and their evolution that illustrate these points well.

5.6.1 Notation

We will use the following symbolic notation throughout this section:

- $\dot{M}$ will denote the rate of mass transfer rate
- R_L will denote the Roche lobe radius
- MS will denote 'Main Sequence'
- P will denote the orbital period
- $\dot{M}_E$ will denote the Eddington accretion rate
- q will denote the mass of the donor divided by the mass of the accretor

5.6.2 Example One: Formation of a Detached White Dwarf and Main Sequence Post Common Envelope Binary

In this situation, we are beginning with a $1.20M_\odot$ star on the left and a $0.80M_\odot$ star on the right. Calculating q we see that it is *larger* than $5/6$ and so from our discussion previously, the mass transfer is **unstable**.

Thus, the timeline goes as follows. Star one (on the left) ascends tehe red giant branch over the main sequence time. As it does this, it begins to expand and fill its Roche lobe. Once the Roche lobe has been filled, mass transfer can begin. But since this mass transfer is unstable, the orbit shrinks and so does the Roche lobe, leading to more mass transfer and the runaway process that was highlighted. This forms a **common envelope** around the binary, which is essentially a 'cocoon' of material surrounding the binary system. This arises from the fact that matter from star one is splling onto star two, but as at this point star two has reached its Eddington luminosity, it is not able to accrete this matter. This leads to the matter surrounding the binary instead. As the stars orbit within this common envelope, the friction of the material leads to significant losses in

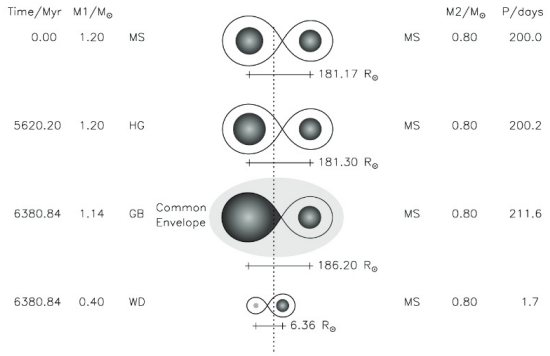

Figure 33: Timeline of Example One

both energy and angular momentum. This results in the two stars getting much closer to one another. Finally, the motion ejects this common envelope and leaves behind a detached binary comprised of a white dwarf and main sequenece star where there is now **no mass transfer**.

5.6.3 Example Two: Formation of a Millisecond Pulsar

Here, we have a much more massive star ($15M_{\odot}$) as star one. This means this star will have a significantly shorter lifespan in comparison. As it ascends the giant branch, its mass decreases by a noticeable fraction due to the strong winds present around massives stars. At this point we have a similar scenario to example one, where star one

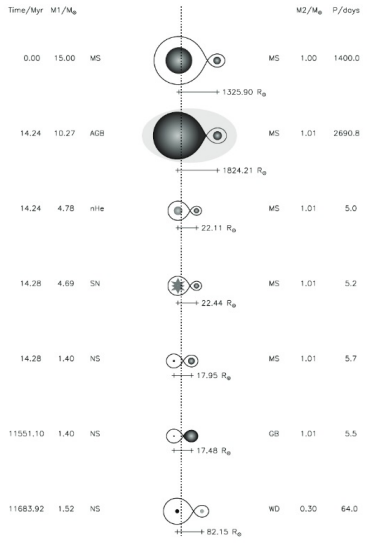

Figure 34: Timeline of Example Two

has expanded to fill its Roche lobe and so has begun transferring mass to star two in an unstable manner (since $q > 5/6$). But once again, star two reaches its Eddington luminosity and so cannot accept any more material which leads to the formation of

a common envelope. Note that in this case, $\dot{M}$ is very close to $\dot{M}_{E,2}$ and so there is very little accretion onto star two. As before, the common envelope is expelled by the motion of the stars leaving behind the helium core of star one. This core then fuses helium into carbon and oxygen, which subsequently gets fused into silicon which is then eventually fused into iron. At this point, via the mechanism described previously in the course, the star explodes as a core-collapse supernova.

At this point, there is a neutron star and a main sequence star orbiting in a binary. This state exists for a long time, as the main sequenece star is much lower in mass and so has a much longer lifespan. But eventually, this star fills its Roche lobe as it ascends the giant branch. This means mass transfer begins but in this instance, $q < 5/6$ so the mass transfer is **stable**. The neutron star gains mass and star two eventually becomes a white dwarf. Note that the mass transfer here is *not* conservative as some of the mass gets blown off by winds or jets.

In the end, the system is left as a neutron-star and white dwarf binary where the neutron star is rapidly spinning (with the period on the order of milliseconds, hence the name). This rapid spinning came from the accretion from star two accelerating the spin period.

5.6.4 Example Three: Two Common Envelopes - Formation of White Dwarf-White Dwarf Binaries

In this situation, we consider three different binaries. All of these have an initial mass ratio of approximately one and a period on the order of a few months. All have the same overall process: One star evolves, eventually filling its Roche lobe and creating a common envelope before expelling it and leaving behind a white dwarf. The other star then does the same process, creating another common envelope and leaving behind a white dwarf as well. Thus, after these two common envelope phases a double white

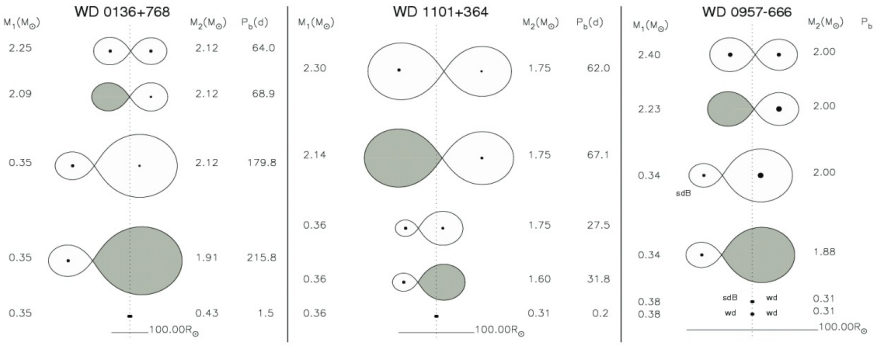

Figure 35: Timeline of Example Three

dwarf binary system remains with an orbital period ranging from hours to days. This short orbital period is due to the common envelope phases and the loss of angular momentum. Eventually, the two white dwarfs will **merge** and if the sum of their masses is greater than the Chandrasekhar limit ($1.4M_{\odot}$) then the merged object will explode as a type Ia supernova.

5.7 Stable Mass Transfer

We end this section on binary systems by discussing stable mass transfer in further detail. Recall that the rate of change of Roche lobe radius has the following proportionality

$$\frac{\dot{R}_2}{R_2} \propto \left(\frac{5}{6} - q\right)$$

Thus, when $q < 5/6$ the orbit and Roche lobe radius R_2 both increase, resulting in the cessation of mass transfer as the donor no longer fills its Roche lobe. This is what we defined as stable mass transfer.

However, for mass transfer to continue, orbital angular momentum needs to be **extracted** from the system so that the orbital separation and the Roche lobe of the donor can decrease. How this angular momentum is lost is the subject of the rest of this section.

5.7.1 Mechanisms of Orbital Angular Momentum Loss

We are going to discuss two ways that orbital angular momentum can be lost from this system. The first method we will describe is extraction via **gravitational waves**. As the two large masses orbit one another closely, general relativity dictates that gravitational waves will be produced. These waves can then carry away angular momentum from the binary. The rate at which this occurs, denoted $\dot{J}_{\rm GR}$, is given by the expression

$$\dot{J}_{\rm GR} = -\frac{32G^{7/3}}{5c^2} M_1^2 M_2^2 (M_1 + M_2)^{-2/3} \left(\frac{2\pi}{P}\right)^{7/3}$$

From this equation, we can immediately tell that the rate at which this occurs is strongly dependent on the mass and the orbital period. In particular, note that as P decreases, the rate of transfer of angular momentum via gravitational waves increases, leading to even further shortening of the period. Thus, a runaway effect occurs until the two objects merge.

Note that transfer of angular momentum in this way occurs in all binaries, but it is not the primary way for most and is rather inefficient in low mass systems or those with longer periods.

The actual timescale on which orbital decay occurs is given by the equation

$$\tau_{\rm GR} = \frac{J}{\dot{J}} = 3.8 \times 10^{11} \frac{(M_1 + M_2)^{1/3}}{M_1 M_2} P^{8/3}$$

where the period P is given in days and $\tau_{\rm GR}$ is expressed in years.

The second means by which angular momentum is lost and the primary method for most stars is via **magnetic (wind) braking**. Consider a rotating star which possesses a dipole magnetic field[8]. Mass is lost in an ionised stellar wind, which is necessarily coupled to the magnetic field of the star is it escaping from. The magnetic field lines rotate at the same frequency that the star spins at. Thus, as the wind moves further out it must increase its velocity to match the spin of the star. This leads to a significant increase of angular momentum which is eventually carried away by the wind as it escapes into space. The point at which the wind is able to escape this magnetic confinement (or

[8]Note that as the name implies, this process does not occur for objects which do not have a magnetic field.

when the Ram pressure of the wind is equal to said magnetic confinement) is referred to as the **Alfvén radius**.

The actual value for the angular momentum is given by the standard expression

$$J = m\omega r^2$$

which implies that this is a very efficient means of angular momentum loss. Note that ω is constant up until the Alfvén radius.

In a binary system, the spin period of the donor is 'locked' to the period of the orbit i.e.

$$P_2 = P_{\text{Orb}}$$

Thus, as the angular momentum is extracted from the donor via the wind, its period and hence its orbital separtion decreases which in turn leads to the spin of the donor decreasing as well. The timescale on which the orbit of a binary system decays due to magnetic breaking is given by

$$\tau_{\text{MB}} = \frac{J}{\dot{J}} = 2.2 \times 10^9 \frac{M_1}{(M_1 + M_2)^{1/3}} r_2^{-4} P^{10/3}$$

from which we can tell that there is a very strong dependence on period for this type of angular momentum loss.

6 Accretion Physics

This section of these module notes will be completed in due time. Until then, the relevant information can be obtained from the lectures given between the 14th and 22nd of February 2024.

6.1 Accretion Discs

[TO BE WRITTEN]

6.1.1 Initial Definitions

[TO BE WRITTEN]

6.1.2 Accretion Disc Formation

[TO BE WRITTEN]

6.1.3 Radial Temperature of the Disc

[TO BE WRITTEN]

6.1.4 Maximum Temperature of the Disc

[TO BE WRITTEN]

6.1.5 Vertical Structure

[TO BE WRITTEN]

6.2 Boundary Layers

[TO BE WRITTEN]

6.3 Angular Momentum Transport in Accretion Discs

[TO BE WRITTEN]

6.4 Accretion onto Compact Objects

[TO BE WRITTEN]

6.4.1 Magnetic Stars

[TO BE WRITTEN]

6.4.2 White Dwarfs

[TO BE WRITTEN]

6.4.3 Neutron Stars

[TO BE WRITTEN]

6.5 The Alfvén Radius

[TO BE WRITTEN]

6.6 Accretion Columns and Shocks

[TO BE WRITTEN]

7 Neutron Stars and Pulsars

We have already considered these fascinating objects within this course, learning how they arise from core-collapse supernova and how their interaction in binary systems can lead to rapidly rotating variants. Now, we dedicate some time to exploring them and their properties in greater depth.

7.1 Magnetic Fields and Spin Periods of Neutron Stars

The neutron stars that we observe are formed with very high spin rates and large magnetic fields. The natural question is why this is the case.

Neutron stars, in the context of core-collapse supernova that we are considering, are formed from the (iron) core of the massive star that eventually collapses. This iron core has a mass of around $1.4M_{\odot}$, a radius of around 8000 km (which is approximately the size of a white dwarf) and a spin period on the order of thousands of seconds. Thus, it can be seen that the properties of the neutron star that arises will be directly dependent on the properties of the progenitor core.

7.1.1 Magnetic Field

Recall that the flux ϕ of a magnetic field $\mathbf{B}$ through a surface S of area $d\mathbf{A}$ is given by the following expression

$$\phi = \int_S \mathbf{B} \cdot d\mathbf{A}$$

This will be utilised later on.

We know that the magnetic flux is conserved when the collapse occurs and so we have the following expression (assuming we are considering a spherical geometry):

$$4\pi B_{\text{Core}} R_{\text{Core}}^2 = 4\pi B_{\text{NS}} R_{\text{NS}}^2$$

We know that the core collapses to a much smaller radius when it becomes a neutron star, so we can immediately see that the magnetic field of the neutron star is going to much larger for the conservation to be maintained. Typical values for this magnetic field are between 10^8 and 10^{11} T, which is incredibly strong.

7.1.2 Spin Periods

Overall, angular momentum must be conserved within this closed system. Thus, we have the following expression

$$I_{\text{Core}}\,\omega_{\text{Core}} = I_{\text{NS}}\,\omega_{\text{NS}}$$

where I denotes the moment of inertia and ω the angular frequency. Recall that the moment of inertia for a solid sphere is given by

$$I = \frac{2}{5}MR^2$$

and that the period is given by

$$P = \frac{2\pi}{\omega}$$

Substituting these values into the above expression and rearraning gives that the spin period of a neutron star is given by

$$P_{\text{NS}} = P_{\text{Core}} \left(\frac{R_{\text{NS}}}{R_{\text{Core}}} \right)^2$$

For an iron core with a period of 1000 s the neutron star will have a period of around 1.5 ms at its genesis.

7.2 Pulsars

7.2.1 Properties

We begin this subsection by discussing what properties are measured from these objects we dub pulsars. The most striking feature is the period pulses of emission, hence their name. These pulse periods range between 1.4 ms and 8.5 s and are **extremely stable**.

Nevertheless, they are measure to lengthen with time. A change of 10^{-17} to 10^{-13} seconds per second is identified, which corresponds to a characteristic time scale of around 10^7 years.

Finally, note that strong magnetic fields are identified around these objects.

Thus, given these properties, we would like to deduce what kind of objects they are.

7.2.2 Identification

Pulsars are **spinning neutron stars**. These objects are physically compact enough to enable them to rotate as rapidly as what is measured. The enormous momentum present means that the rotation period is very stable. The lengthening of the spin period occurs as they lose angular momentum over evolutionary timescales.

The spin period itself has a lower limit set by the rotational break up velocity. This can be found by balancing centripetal and gravitational acceleration as such

$$\omega_{\text{max}}^2 R = \frac{GM}{R^2}$$

where ω_{max} denotes the maximum angular velocity. But this corresponds to the *minimum* spin period via

$$P_{\text{min}} = \frac{2\pi}{\omega_{\text{max}}}$$

Thus, after rearranging one can find that the minimum possible spin period is given by

$$P_{\text{min}} = 2\pi \sqrt{\frac{R^3}{GM}}$$

Calculating this value for a white dwarf demonstrates a minimum period of around seven seconds, which is too slow. However, a neutrons star, which has a minimum period of around 5×10^{-4} seconds, is acceptable as required.

7.2.3 Case Study: The Crab Pulsar

The first pulsar to be discovered in a supernova remnant was the **Crab Pulsar (PSR 0531-21)**. This proved to be the first connection between neutrons stars and supernovae. Furthermore, this 'dead star' has a luminosity value of around $10^5 L_\odot$. It is natural to then ask what is powering this emission.

Consider the rotational kinetic energy, which is given by

$$E_k = \frac{1}{2} I \omega^2 = \frac{2\pi^2 I}{P^2}$$

The rate at which the neutron star loses energy as it spins down, dubbed the **spin-down luminosity**, is identified by differentiating this expression with respect to time in order to give

$$\frac{dE_k}{dt} = -\frac{4\pi^2 I}{P^3}\dot{P}$$

Inputting standard values for a neutron star gives a spin-down luminosity which corresponds with the value above. Thus, we are able to deduce that pulsars are **rotation powered**.[9]

Now we are going to consider the magnetic field of this pulsar. A magnetic dipole that is rotating on an axis offset from the spin axis of the neutron star will produce **magnetic dipole radiation**. The energy emitted from this rotation is given by the following expression

$$\frac{dE}{dt} = \frac{32\pi^5 B^2 R^6 \sin^2(\theta)}{3\mu_0 c^3 P^4}$$

If we assume that all the energy from the reduction in spin is transferred away via this dipole radiation, then we can set this expression equal to the boxed one above and rearrange to get

$$B = \frac{1}{2\pi R^3 \sin(\theta)} \sqrt{\frac{3\mu_0 c^3 I P \dot{P}}{2\pi}}$$

For $\theta = 0^\circ$ this gives a value of around 8×10^8 T. In reality, the actual value is about half this as other loss mechanisms are present.

7.3 The Lighthouse Model

We can model pulsars using the **Lighthouse model**, which we are going to discuss now. A diagram of a pulsar is below. We are considering a strongly magnetic and rotating neutron star with a spin axis that is **misaligned** with the magnetic axis. As the plasma surrounding the pulsar rotates through the magnetosphere, Faraday induction generates a very large electric field at the surface of the neutron star.

At the poles, this electric field is sufficiently strong for the charged particles present there to be able to overcome the gravitational force of the neutron star and accelerate away. This leads to jets being expelled from either pole of the neutron star. As the pulsar rotates, the jets sweep across the line of sight of an observer, leading to a periodic flash. Furthermore, any charged particles travelling along the field line will be forced to rotate at the same frequency as the neutron star/pulsar. This rotational velocity will

[9] The specific details of this are not entirely well understood.

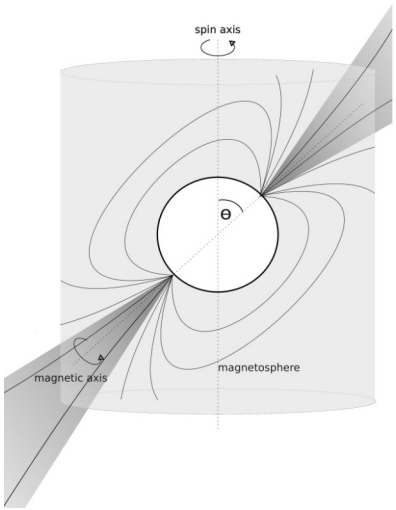

Figure 36: The Lighthouse Model of Pulsars

increases the further away from the neutron star the particle gets. At a radius called the **light cylinder radius**, the Ram pressure of the particles is greater than the magnetic field strength and so the particles are able to escape. This means that over time **isolated pulsars will spin down** as the open field lines effectively 'slow' the neutron star down.

7.4 Period-Period Change Diagrams

By observing a pulsar over a period of time, astronomers are able to measure its period and the change its period. Plotting these on a period-period change diagram is very useful, as from this many properties of the pulsar can be determined. For example,

- Age $\propto P/\dot{P}$
- Magnetic field $\propto \sqrt{P\dot{P}}$
- Spin down luminosity $\propto \dot{P}/P^3$

Consider the logarithmic period-period change plot below. There are several things to discuss about this plot. Firstly, observe that as the x-axis increases, the spin period is longer and as the y-axis increases, the pulsar spins down faster and has a higher magnetic field.

The timeline of a typical pulsar can be viewed as moving over this diagram. Pulsars that are recently 'born', such as Crab and Vela, are in the top region spinning quickly and with a high magnetic field. Over time, they spin down and their magnetic field decreases meaning they move down the plot. This leads to the region where the majority of pulsars lie. However, *isolated* pulsars will continue to spin down and eventually return to being regular neutron stars leading them to fall into the **graveyard** region. They are now very difficult to detect, as they no longer send out identifiable jets. This is the evolution for the bulk of pulsars.

However, there are other objects of note on this plot. The first is those in the top right, comprised of very slowly spinning objects that have incredibly high magnetic fields. These are referred to as **magnetars** and are not very well understood. The second

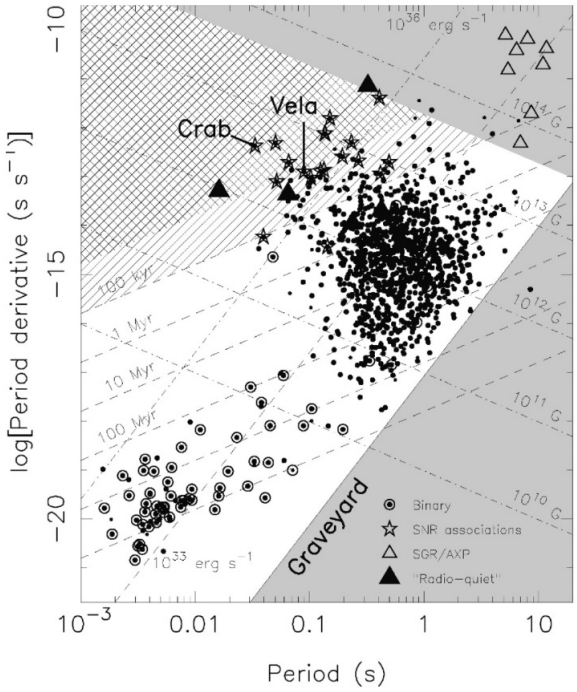

Figure 37: Period-Period Change Diagram

are those in the bottom left which have low magnetic fields but incredibly high spin periods. These are the **millisecond pulsars** previously discussed, which are pulsars in binaries that have had their spin sped up via mass transfer. We devote the final part of this section to discussing these objects.

7.5 Millisecond Pulsars

Here, we want to directly confirm that mass transfer is enough to spin up a neutron star to the millisecond regime. Recall that the orbital angular momentum of a binary system is given by the following expression

$$L_{\Omega,i} = M_{\mathrm{NS},i} M_{\mathrm{Donor}} \left(\frac{Ga}{M_{\mathrm{NS,i}} + M_{\mathrm{Donor}}} \right)^{1/2}$$

where the i denotes **initial**. Furthermore, the spin angular momentum of the pulsar (if a solid sphere is assumed) is given by

$$L_{\omega} = I_{\mathrm{NS}} \omega_{\mathrm{NS}} = \frac{2}{5} M_{\mathrm{NS}} R_{\mathrm{NS}}^2 \omega_{\mathrm{NS}}$$

Let the mass transfer from the donor to the neutron star be conservative, recalling that this means that all matter is transferred to the neutron star and none is lost. The highest spin rate that the pulsar can achieve is the situation where *all* the angular momentum of the binary system were to be transferred to the angular momentum of the pulsar i.e.

$$L_{\Omega,i} = L_{\omega,f}$$

Thus, setting these expressions equal and rearraning gives the following expression for the final angular momentum of the neutron star as

$$\omega_{\mathrm{NS},f} = \frac{5}{2}\frac{M_{\mathrm{NS},i}}{M_{\mathrm{NS},f}}\frac{M_{\mathrm{Donor}}}{R_{\mathrm{NS},f}^2}\left(\frac{Ga_i}{M_{\mathrm{NS},i}+M_{\mathrm{Donor}}}\right)^{1/2}$$

Let us use this expression to see if this expression confirms our hypothesis. Consider a binary consisting of a typical neutron star with mass $1.4M_\odot$ and a radius of 10 km and a donor star with mass $0.8M_\odot$ where the period of the orbit is 80 minutes, corresponding via Kepler's third law to a separation of 4.9×10^8 m. Recall that for degenerate matter, we have the following proportionality relation

$$R \propto M^{-1/3} \implies \left(\frac{M_{\mathrm{NS},f}}{M_{\mathrm{NS},i}}\right)^{-1/3}$$

Thus, the final radius of the neutron star is 9816 m. Hence, substituting these values into the expression above gives a value of

$$\omega_{\mathrm{NS},f} = 4\times10^5\,\mathrm{rad/s} \implies P = 1.5\times10^{-5}\,\mathrm{s}$$

Thus, accretion can certainly increase the spin period of a pulsar. But whether it be able to reach this spin period without breaking up is the next query.

Recall that the maximum angular frequency, rotating faster than which will cause the break up of the object, is given by

$$\omega_{\mathrm{max}} = \sqrt{\frac{GM}{R^3}}$$

For this neutron star, substituting values in gives a maximum angular frequency of around 14 000 rad/s, corresponding to a minimum spin period of 5×10^{-4} s. Thus, whilst accretion *can* spin this object up it will break apart before its maximum spin period is reached.

8 Black Holes

Earlier in the course, we discussed the creation of black holes of a few solar masses from single star evolution. But as it turns out, there are much larger and more intense black holes out there. In this section, we are going to explore the intense physics of these spectacular objects as well as the methods by which they are identified and imaged.

8.1 Recap of Classification

Recall that in section two we classified black holes into the following three categories based on their mass:

- Stellar mass black holes, which have a mass of between 3 and $\sim$ 100 solar masses. Note that the exact lower limit is unknown.
- Intermediate mass black holes (IMBH), which have a mass between a few 100 solar masses and 10^5 solar masses. The boundary between stellar mass black holes and IMBHs is not well defined. The important thing to note about this class of blac khole is that there is **no definitive detection** of them. However, there is observational and theoretical evidence for their existence.
- Supermassive black holes (SMBHs), which have a mass of between 10^6 and 10^8 solar masses. These are found within the centres of galaxies and their method of formation is unknown.

8.2 Observational Evidence for Black Holes

We are now going to turn out attention to the observational evidence we have that these astrophysical objects actually exist.

8.2.1 Evidence for Stellar Mass Black Holes

There are many pieces of evidence for the existence of these types of black holes. We will discuss some of these now.

The first is the detection of gravitational waves from merging events. From this data the masses of the objects that merged as well as how close they approached before they merged can be calculated. These two pieces of information allow us to infer that black holes are the cause of the gravitational waves.

The next piece of evidence is that in some X-ray binaries, the inferred accretor masses - which can be calculated from the orbital period and Kepler's third law - are too large to be anything but black holes. A key example of this is the black hole Cygnus X-1.

Powerful outflows and high-energy emission from accretion discs in some X-ray binaries are indicators of black hole accretors. Consider a binary system with a black hole. At a point in the accretion disc that is very close to the black hole, the gravitational potential well is *very* deep. From our chapter on accretion physics, this means that very high energy emissions is thus detected. The spectrum of an accretion disc can be used to calculate the mass of an accretor which can in turn indicate the existence of a black hole.

A further line of evidence is the high-frequency variability in light curves of some X-ray binaries, which indicate that the accretion disc extends too close to the accretor for it to be a neutron star.

Finally, if a black hole is moving between an observer and a background star will gravitationally lens the light, making it appear temporarily brighter. This **gravitational microlensing** is another piece of evidence for stellar mass black holes.

8.2.2 Evidence for Intermediate Mass Black Holes

As already stated, there is no direct evidence observational evidence for black holes with this range of mass. The best candidates in this bracket are ultra-luminous X-ray sources (denoted ULXs). These are objects with extremly high X-ray luminosity, on the order of $10^{39}\,\mathrm{Js}^{-1}$. This is much too high to be from any known stellar process. However, it could be produced from accretion onto a compact object.

If we assume that all this X-ray emission is from accretion, then we know the upper limit is the Eddington luminosity. Calculating this, we see that

$$M = \frac{L_{\mathrm{Edd}}\sigma_T}{4\pi GMm_p} \geqslant 1000M_\odot$$

Thus, these ultra-luminous X-ray sources are viable candidates for IMBHs since the luminosity being produced can be explained reasonably by accretion onto an IMBHs.

Note that there are other lines of evidence for these types of black holes, but they are not discussed within this course.

8.2.3 Evidence for Supermassive Black Holes

One of the earliest examples of evidence for this class of black holes is the observed motion of stars in the centre of the Milky Way, which indicates they are orbiting a SMBH.

The arguably more convincing and spectacular evidence is that these objects have been directly 'imaged' by the Event Horizon Telescope (EHT).

A lot of the evidence for stellar mass black holes is applicable to these objects as well, such as the high-frequency oscillations in the light curves of the centre of galaxies, powerful jets and outflows from galaxies and gravitational microlensing.

Two final pieces of evidence for these objects are the **flares** seen from stars being shredded and accreted by SMBHs - which are called **tidal disruption events** - and the the fact that velocity dispersions of stars and gas near the centre of galaxies rises as $1/r$. This indicates a large and highly concentrated mass at the center of the galaxy i.e. an SMBH.

8.3 Sagittarius A* - The SMBH at the Centre of our Galaxy

There is one supermassive black hole which has been studied in great detail and that is the one at the center of very own galaxy, Sagittarius A* which is abbreviated Sgr A*. In this section we are going to delve into more detail about what information we know about this superb object and how we know it.

8.3.1 Resolved Stellar Orbits around Sgr A*

As stated before, one key piece of evidence for the existence of an SMBH is the observed motion of stars around the centre of the Milky Way. But the galactic centre is dusty, faint and incredibly crowded. To effecitvely observe it we need several things working in our favour. These include:

- Infrared observations at long wavelengths in order to see past the dusty material.
- Milli-arcsecond resultion in order to resolve the objects. This requires a delicate use of adaptive optics.
- A telescope with a large aperture.

What is the maximum resolution we can achieve for the galactic centre? Viewing at a wavelength of 1 µm and with a telescope that has an 8 m aperture, we can calculate this using our minimum viewing angle formula from section four. Thus,

$$\Delta\theta = 1.22\frac{\lambda}{D} = 0.03"$$

At the galactic centre we can resolve physical scales of the source size divided by the distance to the source. Putting this together means that we can resolve a distance of 240 astronomical units at the galactic centre.

A program actually monitoring the galactic centre is the Very Large Telescope Interferometer (VLTI). Its observations of the galactic centre over the span of months to years demonstrated that the stars orbit the super massive black hole Sgr A*. One particular star that was monitored has completed more than one orbit since monitoring began in 1994 and so its properties are known to a good degree of accuracy. The orbit of this star has a semi-major axis of $a = 935$au, an orbital period of $P = 15.73$ years and an ellipticity of $e = 0.87$. More orbits have been observed over time and the findings are presented in the figure below. From these values and Kepler's third law, we are able

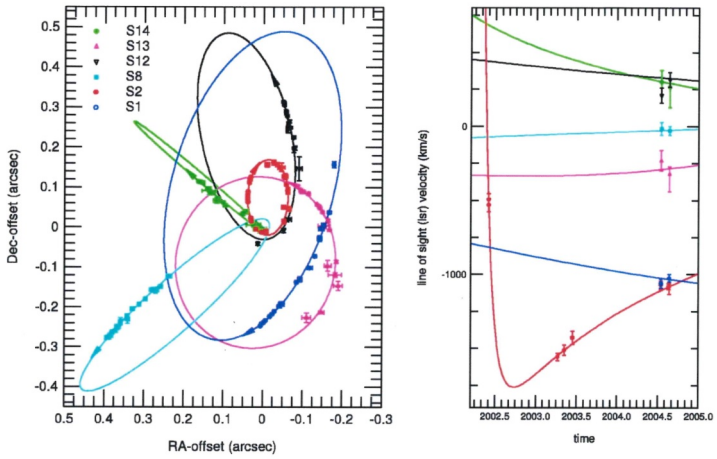

Figure 38: Orbits of the stars around Sgr A*

to reasonably calculate the mass of Sgr A*. Kepler's third law states that

$$P^2 = \frac{4\pi^2 a^3}{G(M_{\text{Sgr A*}} + M_{S_2})}$$

But since $M_{\text{Sgr A*}} \gg M_{S_2}$, we can say that

$$P^2 \approx \frac{4\pi^2 a^3}{GM_{\text{Sgr A*}}} \implies M_{\text{Sgr A*}} \approx 4 \times 10^6 M_\odot$$

At this point, we have not actually confirmed that the stars are orbiting a supermassive black hole. This can also be determined from the orbit of the stars outlined above. To be specific, the distance of closest approach, denoted r_{min} is 6.25 light hours by star S17. We can then put an upper bound on the volume of the object that S17 is orbiting as follows

$$V < \frac{4}{3}\pi r_{\text{min}}^3$$

Thus, the density has a lower bound of

$$\rho > \frac{M_{\text{Sgr A*}}}{V} = 6 \times 10^{-6}\,\text{gcm}^{-3}$$

This density is too large to be explained currently by anything other than a supermassive black hole. Thus, it seems most likely that this is what is at the centre of our galaxy.

8.3.2 Direct Imaging of M_{87}* and Sgr A*

The Schwarzschild radius of Sgr A* can be calculated using the formula derived previously, namely

$$R_{\text{sch}} = \frac{2GM}{c^2} = 0.8\text{au}$$

This is much too small for the infrared 8 metre aperture telescope we considered in the previous subsection, as that gave a maximum resolution of 240au. To be able to resolve this, a resolution of around 10×10^{-6} arcseconds would be required.

The question is whether this is actually feasible. Sgr A* is bright at radio wavelengths, so these will be preferred. It should be noted that for radio the resolution is given by

$$\Delta\theta = 1\frac{\lambda}{D}$$

where the prefactor 1 depends on the wavelength being observed and the shape of the mirror.

The highest resolution telescope is the Event Horizon Telescope, which is a radio telescope operating at 230 GHz, which corresponds to a wavelength of $\lambda = 1.3\,\text{mm}$, and with an aperture of $1.1 \times 10^7\,\text{m}$. This aperture is made possible with the use of **interferometry** (hence the name) which is a technique which combines telescopes together to create higher resolution images. Overall, this means that EHT has a resolution of 25×10^{-6} arcseconds, which is almost enough to be able to resolve the event horizon of Sgr A*.

To this end, EHT has imaged two supermassive black holes. These are Sgr A* and M_{87}*, which is an active galaxy around 55×10^6 light years away from us. The mass of this black hole was able to be derived from this image and came out to be $6.5 \pm 0.7 \times 10^9$ solar masses.

The M_{87}* image is shown below in the X-ray wavelength. We are now going to discuss some key observations. There is a well defined **emission ring**. The hot accretion disc around the SMBH emits light, in particular, synchotron emission at radio wavelengths. This is gravitationally lensed to produce a bright ring of emission at the photon capture radius. There is also the black hole **shadow**. This is the area where the black hole has captured the incoming photons.

The most striking feature is that the lower half of the ring is **brighter**. This is due to the fact that the rotation axis of M_{87}* and the accretion disc is pointed away from us

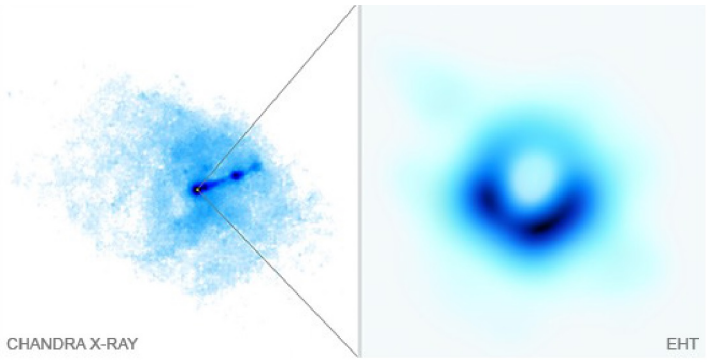

Figure 39: M87 imaged in X-Ray (Note that the colours are inverted)

(197° to our line of sight). Thus, the material in the accretion disc is moving clockwise and, since the the disc is tilted with respect to our line of sight, moving towards us. Close to the black hole this material is moving at relativistic velocities and so a process called **relativistic beaming** makes said material appear brighter. We are now going to discuss this process in more detail.

8.3.3 Relativistic Beaming

Let S be the rest frame of Earth. Consider material that is emitting photons isotropically in its rest frame S'. This material is moving with relativistic velocity v in the x-direction with respect to Earth. Let a photon be emitted at an angle θ' in S'. By performing a Lorentz transformation, we can calculate what angle this will be emitted at in the frame S. We have that

$$v_x = \frac{v'_x + v}{1 + \frac{vv'_x}{c^2}} \quad \text{and} \quad v_y = \frac{v'_y}{\gamma\left(1 + \frac{vv'_x}{c^2}\right)} \quad \text{where} \quad \gamma = \frac{1}{\sqrt{1 - \left(\frac{v}{c}\right)^2}}$$

Thus, the angle observed is given by

$$\tan(\theta) = \frac{v_y}{v_x} = \frac{v'_y}{\gamma(v'_x + v)} = \frac{c\sin(\theta')}{\gamma(c\cos(\theta') + v)}$$

From this, we can see that the angle θ that we see in S is different to the angle θ' that the photon was emitted at in S'.

If we specifically consider a photon emitted in the S' frame at $\theta' = 90^\circ$, then

$$\tan(\theta) = \frac{c}{\gamma v}$$

For velocities approaching the speed of light (i.e. as $v \to c$) then θ will be come very small. In this case

$$\tan(\theta) \approx \theta \approx \frac{1}{\gamma}$$

Thus, the photon is **beamed** in a forward direction (i.e. the direction of travel of the jet). Thus, for an isotropically emitting source, half of the photons - specifically those with $\theta' \leqslant \frac{\pi}{2}$ - will be beamed into a cone with half opening angle $\theta \approx \frac{1}{\gamma}$ in the direction

of motion. Thus, the source appears brighter if we are looking in that direction. The EHT images of Sgr A* also shows the same features that we have discussed about the image of M_{87}*, specifically the shadow and ring structure. An image is provided below. However, in this case the accretion disc is oriented at 40° to our line of sight.

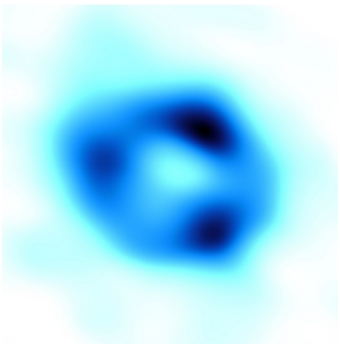

Figure 40: Sgr A* imaged in X-Ray (Note that the colours are inverted)

Thus, the beaming is not as pronounced.

8.4 Location and Masses of Super Massive Black Holes (SMBH)

8.4.1 The M-σ Relation and its Implications

All massive galaxies are believed to harbour a super massive black hole at their centres. The mass of the galaxy and of its SMBH are related via the **M-σ relation**, which is an empirical correlation between the stellar velocity distribution, denoted σ, of a galaxy and the mass of its SMBH. The expession has the form

$$\frac{M_{\text{SMBH}}}{10^8 M_{\odot}} \approx 1.9 \left(\frac{\sigma}{200\,\text{kms}^{-1}} \right)^{5.1}$$

A plot of the masses of some galaxies plotted against their stellar velocity dispersion is shown in figure [41] below. Note that the velocity dispersion is measured via measurement of the redshift of the spectral lines. As stellar velocity dispersion increases, the mass of the galaxy increases. The logical question is why such a correlation exists. The answer lies in the **Virial theorem**. In a gravitating system in hydrostatic equilibrium, the total gravitational potential energy E_p is related to its kinetic energy E_k via the following expression

$$E_k = -\frac{1}{2} E_p$$

Thus, if we measure the total mass of a galaxy out to a radius r, then

$$\frac{1}{2} m \langle v^2 \rangle \approx \frac{1}{2} \frac{GMm}{r}$$

where m is the typical mass of a body and $\langle v^2 \rangle$ is the mean velocity squared with respect to the centre of mass. Cancelling terms then demonstrates that

$$\langle v^2 \rangle = \frac{GM}{r}$$

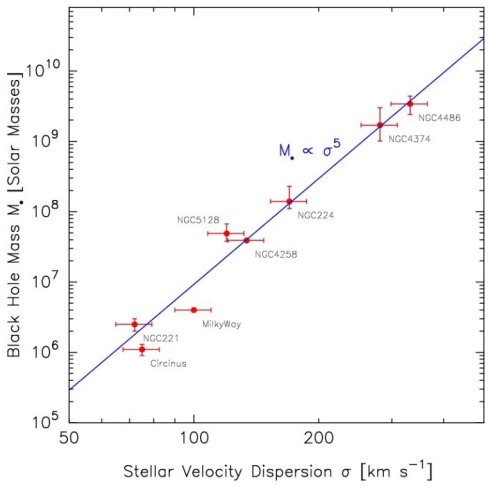

Figure 41: M-σ Relation Plot

Thus, there is a direct correlation between the mass of the SMBH at the centre and mean velocity squared as described by the M-σ relation.

There are two main implications of this result. The first is that the tight correlation indicates that **all** massive galaxies likely have an SMBH at their centre. The second is that the same tight correlation indicates that the evolution of a galaxy and its SMBH are fundamentally linked[10].

8.5 Active Galactic Nuclei (AGN)

8.5.1 Initial Description and Discussion

We are now going to consider a special class of super massive black holes. In some galaxies, the accretion rate of the SMBH is low. This means that their centres are comparatively faint and do not drive powerful jets. Such SMBHs are dubbed **inactive**.

In contrast, other galaxies have a SMBH where the accretion rate is so high that their cores are extremely luminous and drive incredibly powerful jets. The inner regions of these **active** galaxies are called **active galactic nuclei** or **AGN**, which we will spend the remainder of this section discussing.

To begin, we perform an initial illustration and description the structure of an AGN in the figure below. Firstly, there are **jets** which are **radio bright** and typically hundreds of kiloparsecs long. At the ends of these jets, there are **jet lobes**, which are bright sources of synchotron emission that arise from the shockwaves caused by the collision of the jet with material within space.

Next, the inner region is comprised of a supermassive black hole at the centre with an **accretion disc** surrounding it. Around this there is an **obscuring torus** which is comprised of **dust** that surrounds the galaxy. This indicates that the angle at which we observe an AGN will determine how much light we see from the centre.

Finally, there are two areas called the **broad line region** nearer the accretion disc and the **narrow line region** further away.

[10]This is explored more in the fourth year physics course PX444: The Distant Universe

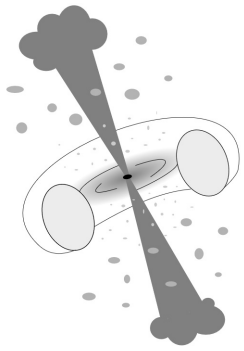

Figure 42: Illustration of an AGN

8.5.2 Argument that AGN are powered by SMBH

To confirm that supermassive black holes are the objects actually powering the active galactic nuclei we can make the following argument.

When measured, the luminosity of the inner region of galaxies varies significantly over the course of a few days. This means that the time for light to travel across the diameter of the source is less than or equal to a few days. If this was not the case, then the luminosity detected would be 'smeared out' by the delayed arrival times of photons from more distant regions. The size of the central object, denoted l, is limited by

$$l \leqslant c\Delta t$$

Thus, for a variability of an example value of 10 days, then $l \leqslant 3 \times 10^{14}\,\mathrm{m}$ which is around 2000 astronomical units. The luminosities for AGNs are around 10^{11} to $10^{15} L_{\odot}$ which is about a thousand times brighter than the luminosity of the Milky Way. Since this huge power output is coming from such a comparatively small area, the only reasonable explaination is that an accreting black hole is powering the AGN.

8.5.3 Components of an AGN

We are now going to discuss the components of an AGN that were described previously in more detail.

Firstly, we consider the **obscuring torus**. This is a large scale structure comprised of dust which surrounds the accretion disc. Depending on the line of sight, this can **block the AGN** in which case the black hole and accretion disc are not observable. The high energy emission from the accretion disc, which is in the ultraviolet and X-ray wavelengths, is abosrbed and reradiated as infrared emission by the dust.

The **broad line region** is composed of clouds within around $10^{14}\,\mathrm{m}$ of the black hole (which is within the torus). These clouds are heated to $10^{4}\,\mathrm{K}$ by the ionising radiation from the accretion disc. They have velocities of approximately $5000\,\mathrm{km/s}$, resulting in large Doppler shifts for individual clouds. Collecting these measurements together for the whole region produces broad spectral lines, thus, the name.

The **narrow line region** is comprised of more distant clouds with smaller velocities and thus the collect spectral lines are narrower.

Jets, as we described, are collimated outflows of ionised materials aligned along the rotation axis of the accretion disc i.e. perpendicular to the disc itself. These jets move

at relativistic speeds and eventually collide with material which results in large **shocks** that radiate synchotron emission and inverse-Compton emission. These regions at the 'ends' of jets are referred to as **jet lobes**. It is important to note that jets are *not* unique to AGN and fairly common, found in many accreting systems such as X-ray binaries, newly forming stars and more.

8.5.4 The Launching Mechanism of Jets - The Blandford-Znajek (BZ) Process

Currently, the method by which jets are launched out of the centre is not well conclusively known. However, there are some key models about how this may occur and one of these for black holes is known as the **Blandford-Znajek (BZ) process**.

This model requires a **spinning black hole** and a surrounding ionised accretion disc with a **strong poloidal magnetic field**. The accretion onto the black holes drags the magnetic field lines in the inner disc closer to the black hole, thereby threading them through the event horizon, whilst the other end is threaded through the disc.

However, there are relativistic factors at play as well. The spinning of the black hole causes local space-time to rotate in the same direction as the black hole. This is the relativistic frame dragging we discussed previously and is illustrated in the figure below This frame dragging causes the magnetic field lines to twist and form loops, as the

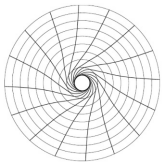

Figure 43: Threading of magnetic field lines

inner end of the filed line is rotating faster than the outer end. This results in a **toroidal magnetic field**, which exerts a magnetic pressure thereby pushing the surrounding material out of the inner disc and forming the jet. This mechanism is presented in the figure below. Note that the energy for this is coming from the **rotational energy** of the black hole.

Figure 44: Formation of a toroidal magnetic field

8.5.5 Superluminal Motion

To end this section, we will discuss and explain the observation that clumps in the jet appear to move away from an active galactic nuclei over time. An example of this is presented in the figure below, which shows the evolution of the jet present in 3C273 over time. The luminosity is denoted by the contours on the plot and the left 'blob'

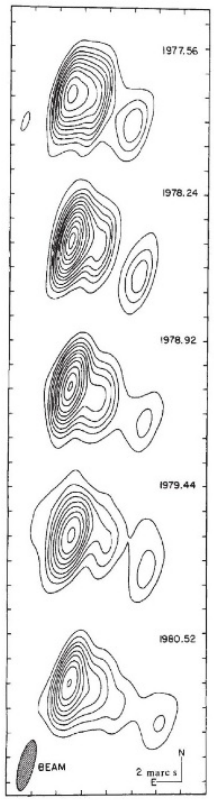

Figure 45: Evolution of the jet of 3C273 over time

denotes the active galactic nuclei and the right one denotes the jet. Over time, one can see, as stated, that the jet love appears to move further away from the AGN.

Recall that **proper** or **transverse motion** is defined as the velocity component perpendicular to the line of sight of the observer. For this plot, the transverse angular velocity, which can be calculated as the change in angle over time, is around 0.0008 arcseconds per year. We can use this value to calculate the apparent velocity of the jet given that the distance to 3C273 is around 312Mpc. The jets will move a distance

$$\Delta r = d\Delta\theta$$

and so the apparent velocity of the jets is given by

$$v_{\text{app}} = \frac{\Delta r}{\Delta t} = \frac{d\Delta\theta}{\delta t}$$

Substituting the values we have found means that this apparent velocity comes out to be around 7.85 times the speed of light. This apparent paradox, where the apparent

velocity is larger than the speed of light, is called **superluminal motion**[11].

To explain this, consider a compact object at a distance d from Earth which launches a relativistic jet with velocity v at an angle ϕ with respect to the line of sight of the observer. Within this jet are 'knots' of material which are moving along the jet at the velocity of the jet.

Let one knot emit a photon (dubbed photon one) into our line of sight at time $t = 0$. At a later time $t_e > 0$, assume the knot emits another photon (dubbed photon two) also into our line of sight. We thus have arrangement represented diagramatically below. The distance travelled by the knot from A to B is simply vt_e. Using trigonometry we

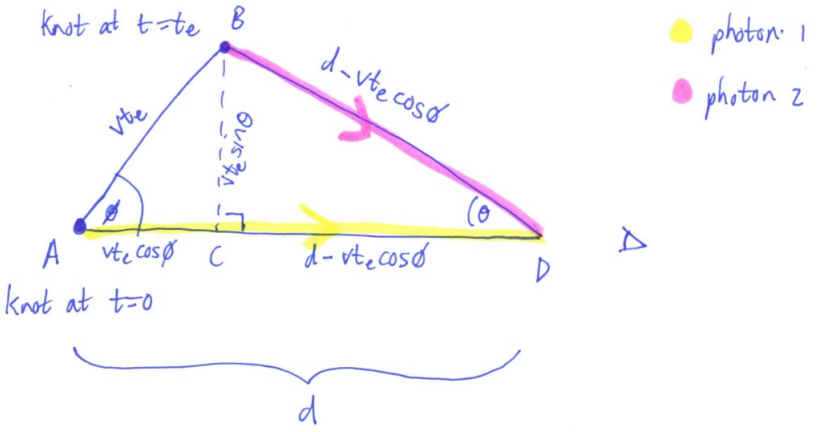

Figure 46: Emission of photon one and two from the knot

can get the following identities for the different distances:

$$AC = vt_e\cos(\phi) \quad ; \quad BC = vt_e\sin(\phi) \quad ; \quad CD = d - vt_e\cos(\phi)$$

The angle between teh two incident photons, denoted θ in the diagram, is small. Hence, using the small angle approximation we can say that the distance travelled by photon two is given by

$$BD \approx CD = d - vt_e\cos(\phi)$$

Therefore, we know that photon one will arrive at Earth at time

$$t_1 = \frac{AD}{c} = \frac{d}{c}$$

and photon two will arrive at Earth at time

$$t_2 = \frac{BD}{c} + t_e = \frac{d - vt_e\cos(\phi)}{c} + t_e$$

The time between the photons arriving at Earth is thus given by

$$\Delta t = t_2 - t_1 = t_e\left(1 - \frac{v}{c}\cos(\phi)\right)$$

and so the transverse velocity can be calculated by the expression

[11] Note that this shown by other objects as well, such as the black hole MAXI J1820+070.

$$v_{\text{tr}} = \frac{BC}{\Delta t} = \frac{v t_e \sin(\phi)}{t_e \left(1 - \frac{v}{c}\cos(\phi)\right)} = \frac{v \sin(\phi)}{1 - \frac{v}{c}\cos(\phi)}$$

This explain the paradoxical result. As the jet is moving at an angle ϕ with respect to the line of sight of the observer, photon two will be emitted closer to them and thus have to travel a shorter distance than photon one. Consequently, a shorter time will be measured between the photon arrival times and thus a higher velocity is measure as well. If the jet speed was already a signficant fraction of the speed of light, then the measure apparent velocity would appear to go over it. The jet velocity is approximately equal to the escape velocity i.e.

$$v_{\text{jet}} \approx v_{\text{esc}} = \sqrt{\frac{2GM}{R}}$$

and so for black holes this value is always approximately equal to the speed of light no matter the mass of the black hole since the Schwarzschild radius scales as a function of mass, as does the escape velocity. Hence, this effect is always applicable when considering jets being expelled from black holes.

9 Gravitational Waves

Our final section within this course will be discussing gravitational waves, which as one may recall was one of the mechanisms via which angular momentum was transferred out of binary systems. Gravitational waves are at the forefront of physics, having only been detected directly fairly recently. Lots of discoveries are being made within this subfield and they are of incredible importance to the new era of astrophyiscs research. We will discuss what they are, how they arise from certain stellar systems and the means by which they are able to be detected.

9.1 Definitions and Properties

Gravitational waves are **ripples in space-time**, or changes in the curvature of space-time, which arise when masses are **accelerated**. They carry energy and move outwards from their point of creation at the speed of light.

It is of critical importance to note that gravitational waves are **only generated** when the object whose motion is being considered is **not** spherically or rotationally symmetric.

As gravitational waves travel through the Universe, it squeezes space-time in two directions perpendicular to one another *and* to the direction of motion. This means that when observing along the axis perpendicular to the motion of a gravitational wave, one would see the distance between objects **increase** and **decrease** with a **steady cadence**.

Gravitational waves are waves, as the name implies, and thus have the following values:

(i) **Amplitude** or **Strain**: This is denoted by h and is the fraction by which space-time is stretched or compressed. Recall that strain is given by the change in length divided by the original length.

(ii) **Frequency**: Denoted by f

(iii) **Wavelength**: Denoted by λ

(iv) **Speed**: Which has mentioned is the speed of light c

(v) **Polarisations:**[12]

9.1.1 Sources of Gravitational Waves

As previously discussed in section five, orbiting binary stars produce gravitational waves. However, there are many other places where they are generated. These include the following

- Mergers of compact object binaries
- Supernovae (Since their explosions are not in reality perfectly symmetric)
- So-called **primordial gravitational waves** from inflation of the Universe
- Rotation of aspherical neutron stars
- Many others that have two low of an amplitude to be detected with present-day equipment

[12] These are not covered within this course.

The diagram below labels different generators of gravitational waves and the detectors that are being used to identify them. The y-axis denotes the amplitude of the gravita-

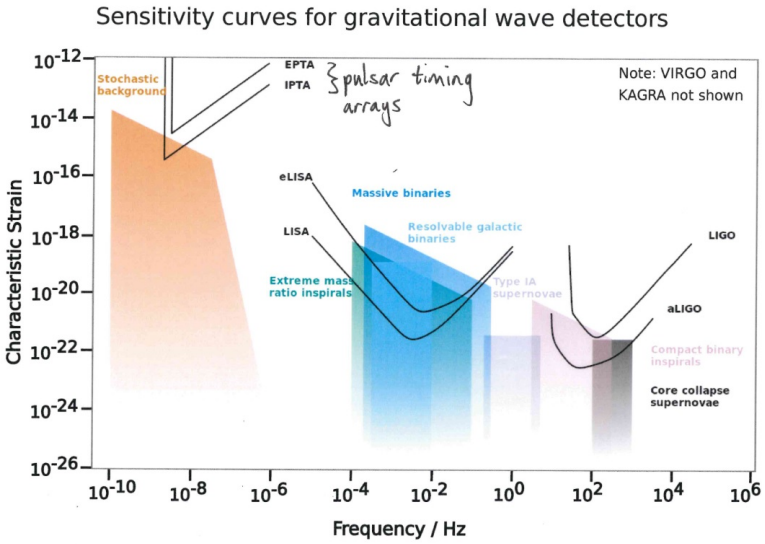

Figure 47: Different source of gravitational waves and relevant detectors

tional wave and the x-axis denotes the frequency. The low frequency section, labelled as 'Stochastic Background' in the plot, denotes progenitors such super massive black holes, active galactic nuclei, cosmic inflation and other similar sources. In the middle are the compact object binaries that orbit one another. White dwarf binaries will be particularly strong emitters within this region. At around one 1 Hz are the gravitational waves produced by type Ia supernovae which were discussed previously in the course. Finally, on the right hand side in the higher frequencies are merger events, specifically merging neutron stars and black holes. The lines themselves show the different **sensitivity thresholds** for the various gravitational wave detectors that are in operation around the world.

9.2 Frequency and Amplitude (Strain) of Gravitational Waves

The intuition for the frequency of a gravitational wave is fairly familiar. The strain on the other hand is a bit harder to interpret and so we devote a discussion here to explaining what is meant by this a bit more in depth.

9.2.1 Single Accelerating Objects

As stated previously, strain is defined as the change in length over the original length, or $\Delta L/L$. A reasonable (Newtonian) approximation for the gravitational strain of a **single** accelerating object at a distance r away is the following equation

$$h \approx \frac{GM}{c^2} \cdot \frac{1}{r} \cdot \left(\frac{v}{c}\right)^2$$

where M and v are the mass and the velocity respectively of the object producing the gravitational waves. From this expression we can see that a larger mass and higher velocity both correspond to a larger strain but note that it decreases with a factor $1/r$ in contrast to the usual inverse square law that is familiar to us from electromagnetic radiation. This means that gravitational waves can travel much further through the Universe and still be detected when compared to electromagnetic waves.

Consider the units of h. By performing dimensional analysis, we can see that the first term GM/c^2 has units of length $[L]$ and the second term $1/r$ clearly has units of $[1/L]$. The third term is a velocity divided by a velocity and so is unitless. Thus, since h is a strain and so is defined by $\Delta L/L$, we get that h is in fact unitless.

9.2.2 Binary Systems

An approximation for the characteristic gravitational strain of a **binary**, with total mass $M = M_1 + M_2$, orbital period P at a distance r is given by the expression

$$h \approx 10^{-22} \left(\frac{M}{2.8M_\odot}\right)^{5/3} \left(\frac{0.01\,\mathrm{s}}{P}\right)^{2/3} \left(\frac{100Mpc}{r}\right)$$

From a binary, the frequency of the gravitational waves produced are **twice** the orbital frequency i.e.

$$f_{\mathrm{GW}} = 2f_{\mathrm{orbit}}$$

And, as for waves in general, the wavelength is given by

$$\lambda = \frac{c}{f_{\mathrm{GW}}}$$

If we consider a specific example, where two $20M_\odot$ black holes in an orbit with a semi-major axis of $4R_{\mathrm{sch}}$ and period of $0.019\,\mathrm{s}$ are located 340Mpc away, then the gravitational waves produced would have a frequency of $105\,\mathrm{Hz}$, a wavelength of $3 \times 10^6\,\mathrm{m}$ and a strain of approximately 1.6×10^{-21}.

This is an incredibly small value for what is quite a major event. Thus, in order to detect gravitational waves directly an elaborate and delicate setup must be concocted. How this is done is the subject of the final section of this course.

9.3 Detection of Gravitational Waves

9.3.1 Indirect Detection of Gravitational Waves

Firstly, let us discuss how gravitational waves may be **indirectly** detected.

The first detection was due to Russell Hulse and Joseph Taylor, who won the 1993 Nobel Prize for their discovery of the binary pulsar PSR1913+16. This enabled for the indirect detection of gravitational waves since the decrease in orbital period measured from this binary system exactly matched the rate predicted by general relativity. This proved that the binary system was emitting gravitational waves.

The second was as a result of **Pulsar timing arrays**, which measure the timing of pulses from many pulsars across the Universe. Gravitational waves will alter the distance to the pulsars and thus change the arrival times of the pulses. These arrays made the first tentative detections in 2023 of the gravitational wave background.

9.3.2 Direct Detection of Gravitational Waves

Here we describe how gravitational wave detectors work by using LIGO as the specific example. An illustration of the setup is presented below To begin, a very powerful

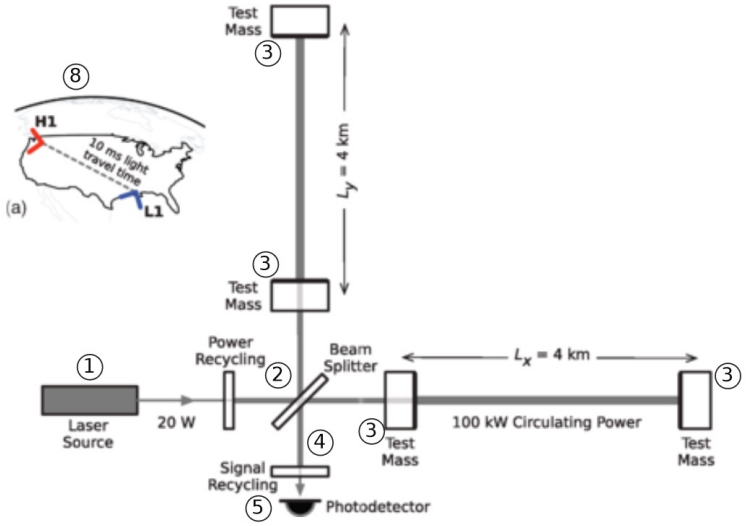

Figure 48: LIGO Setup (Adapted from Abbott et al.)

infrared laser (at position 1) is produced and shone into a vacuum chamber. The beam is then split into two by the **beam splitter** (at position 2), with each one being directed into one of the two vacuum chambers which are of equal length and at 90° to one another.

Each beam is then reflected back and forth several hundred times by mirrors at either end of the vacuum chamber in order to artificially increase the distance of the arm to get a better measurement. Eventually, the beam is combined and shone into the photodetector, which measure the luminosity.

If a gravitational wave **did not** move through the detector during the measurement, then space-time will not have been distorted and thus the light beams will have travelled exactly the same distance. Thus, constructive interference will be seen.

However, if a gravitational wave **did** move through the detector then one arm will shortened or lengthened relative to the over. The two beams would consequently have travelled different distances and hence be out of phase, resulting in deconstructive interference.

If this was only done at one gravitational wave detector, then there would be very little spatial information about *where* the gravitational wave is coming from. Combining multiple detectors allows for the triangulation of the signal based on the time delay between detections and thus the location of generation of the gravitational waves can be calculated.

Note that this setup is *extremely* sensitive to any other kind of disturbance. All possible sources of noise have to be accounted for and limited as much as possible. The mirrors themselves are held up on an intricate system of pendulums and coated in special refelctive coatings to best minimise the impact of any interference.

The first *direct* detection of gravitational waves were from the binary black hole

merger GW150914. As this was the event that led to the detection, we will discuss the stages of it in some detail now.

There are three stages of a black hole merger. These are

(i) Inspiral (where the orbit decreases)

(ii) Merger

(iii) Ringdown (where the new black hole 'settles' into an equilibrium)

The following figure demonstrates how the strain of the gravitational wave being produced as well as the velocity and separation of the black holes varies with time. This is

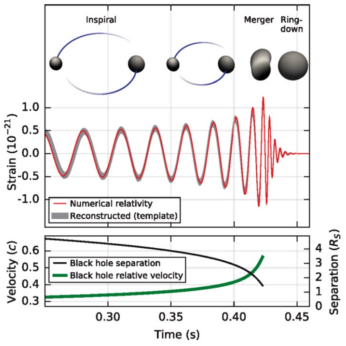

Figure 49: Simulated gravitational wave signal for GW150914

what the ideal signal from a gravitational wave would look like without noise. Notice that as the black holes approach one another to within their Schwarzschild radii and are about to merge, the strain h increases and the frequency f increases rapidly as well. As the merger occurs, the strain and frequency reach a maximum after which they decrease to zero as the ringdown phase arrives.

The actual data from the measurement is shown below The gravitational wave hit Louisiana 6.9 milliseconds before it hit Hanford in this case. The same wave pattern is observed with the residuals appearing to have no pattern, implying that the data was fitted correctly. In the bottom plot, the characteristic **chirp** is demonstrated. As stated, the frequency increased rapidly as the merger occurred with a change of about $600\,\text{Hzs}^{-1}$. The maximum frequency of 150 Hz implies (from analysing [47] shown previously) that this is a compact object merger.

Binary mergers are characterised by the **chirp mass**, which has the following expression

$$\mathscr{M} = \frac{(M_1 M_2)^{3/5}}{(M_1+M_2)^{1/5}} = \frac{c^3}{G}\left[\frac{5}{96}\pi^{-8/3} f^{-11/3}\dot{f}\right]^{3/5}$$

where f is the frequency, $\dot{f}$ is the change in frequency and M_1 and M_2 are the two component masses. We can rearrange this to get that the rate of change of the frequency of a gravitational wave is given by

$$\dot{f} = \frac{96}{5}\pi^{8/3}\left(\frac{G\mathscr{M}}{c^3}\right)^{5/3} f^{11/3}$$

As a specific example, for GW150914 LIGO determined the following values and information:

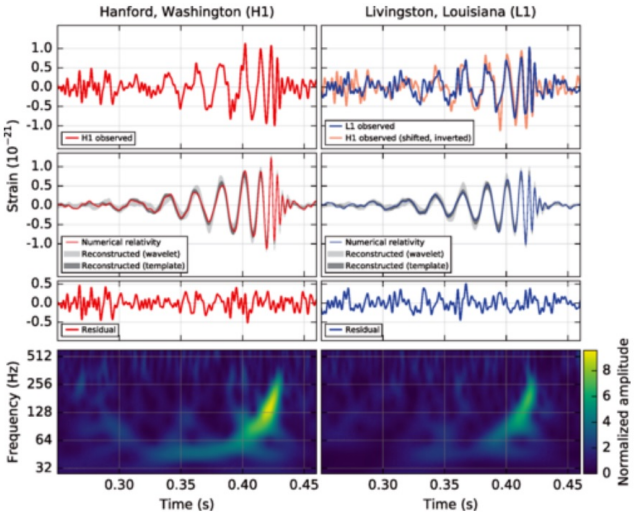

Figure 50: GW150914 Signal recorded by the two LIGO detectors

- $\mathscr{M} = 30M_{\odot}$
- The final Schwarzschild radius was less than 210 km
- The frequency was $f = 150$ Hz so the orbital frequency was 75 Hz
- Signal is consistent with a merger of a binary black hole system leading to a new black hole with a mass of $62 \pm 4M_{\odot}$
- $3M_{\odot}$ of energy was released in the form of gravitational waves

This discovery warranted the 2017 Nobel Prize for Rainer Weiss, Kip Thorne and Barry Barish.

Since this, many more mergers have been detected including the merging of two neutron stars. As more detectors are built and more information acquired, the future of astrophysical research looks to be entering an exciting new era.

A Appendix: Logarithmic Derivatives

Let a be a function of time t. Denote

$$\dot{a} = \frac{da}{dt}$$

as the usual notation. Then since

$$f(a) = \ln(a) \implies \frac{d(\ln(a))}{dt} = \frac{df}{da}\frac{da}{dt} = \frac{\dot{a}}{a}$$

We have that

$$\frac{\dot{a}}{a} = \frac{d(ln(a))}{dt}$$

Now, define

$$a = \frac{b^n}{c^m}$$

where b and c are both functions of time as well. Then consider the time derivative of a as follows

$$\begin{aligned}\dot{a} = \frac{d}{dt}\left(\frac{b^n}{c^m}\right) &= nb^{n-1}\dot{b}c^{-m} - b^n m c^{-m-1}\dot{c} \\ &= n\frac{b^n}{bc^m}\dot{b} - m\frac{b^n}{cc^m} \\ &= na\frac{\dot{b}}{b} - ma\frac{\dot{c}}{c}\end{aligned}$$

Thus, we have the following expression which is referred to as the **logarithmic derivative**:

$$\frac{\dot{a}}{a} = n\frac{\dot{b}}{b} - m\frac{\dot{c}}{c} \quad \text{when} \quad a = \frac{b^n}{c^m}$$